CENTRO DE INVESTIGACION Y DE ESTUDIOS AVANZADOS DEL INSTITUTO POLITECNICO NACIONAL

UNIDAD ZACATENCO

DEPARTAMENTO DE CONTROL AUTOMATICO

Decoding grasp types for Brain-Computer Interface oriented to neurorehabilitation

T H E S I S
Submitted by

Benjamin Domínguez Castelazo

In fulfillment of the requirements for the degree of

MASTER OF SCIENCE

in the specialty of Automatic Control

Supervisors:

Dr. Juan Manuel Ibarra Zannatha

Dr. Luis Montesano

Mexico City NOVEMBER, 2017

CENTRO DE INVESTIGACION Y DE ESTUDIOS AVANZADOS DEL INSTITUTO POLITECNICO NACIONAL

UNIDAD ZACATENCO

DEPARTAMENTO DE CONTROL AUTOMATICO

Decodificación de tipos de agarre para Interfaz Cerebro-Computadora con aplicación en neurorrehabilitación

T E S I S
Que presenta

Benjamin Domínguez Castelazo

Para obtener el grado de

MAESTRO EN CIENCIAS

en la especialidad de Control Automático

Directores de la tesis:

Dr. Juan Manuel Ibarra Zannatha

Dr. Luis Montesano

Ciudad de México NOVIEMBRE, 2017

Acknowledgments

I thank God for he has lead my life thus far. The LORD has been for me more than a Friend, Father and Master. For from him and through him and for him are all things.

I want to thank the Consejo Nacional de Ciencia y Tecnologia (CONACyT) for the financial supporting for my master studies through the scholarship and also for the internship at Bit Brain in Zaragoza, Spain. I am deeply honoured to be part of our country's investment in science and technology.

I would like to thank Juan Manuel Ibarra for your guidance during this last year of the master as well as Jessica Cantillo for the time I spent at INR. In a special mention I thank Luis Montesano, Javier Minguez and all BitBrain work-team for the opportunity to be with you and learn from you, for your help, advice and friendship.

I am deeply grateful to my father, my mother and my two brothers; who even they are far at the same time they have always been next to me.

Abstract

This thesis work, introduces our research results in Brain Computer Interfaces (BCI) with application in neurorehabilitation. A Brain-Computer Interface (BCI) decodes motor actions performed by an user directly from brain signals recording. In the area of rehabilitation, motor BCI systems may improve rehabilitation therapies by allowing control robotic ortheses directly from brain commands or sending a Functional Eletric Stimulation (FES) correlated with Central Nervous System activation which is fundamental to succeed in the rehabilitation therapy.

This thesis work consists in a particular decoding task: Decoding the grasp performed in a functional movement comprising reach, grasp and object manipulation; from EEG recording. Two main goals are followed by this thesis: First, we analyse EEG record to find neural correlates of grasping, more exactly, to find Movement Related Cortical Potentials that are neural signatures of movement. The second goal is decoding between force grip and precision grip from EEG signals using MRCP.

For that aim, we designed an experimental protocol, 10 healthy subjects were recorded, records were off-line processing. For both, EEG analysis and grip decoding we implemented and assessed diverse preprocessing and machine learning techniques.

We obtained the following results: Concerning to EEG analysis, we found MRCP signals in grasp funcional movements. Furthermore, we observed some relevant characteristics in temporal evolution of MRCp related to the event they are time-locked. Regarding decoding of grip performed , we exploited features extracted from MRCP using two classifiers, LDA and SVM with radial basis function as kernel. We decode first rest vs grasp with an accuracy of 76.74%. For decoding between force and precision grip, we achieved 64.89 %.

Resumen

En esta tesis se presentan los resultados de nuestra investigación en Interfaces Cerebro Computadora (BCI) orientada a neurorrehabilitación. Las interfaces cerebro-computadora motoras permiten la descodificación de acciones motoras realizadas por un usuario a partir de señales cerebrales. En el campo de la neurorrehabilitación, los sistemas BCI de decodificación motora pueden participar en las terapias de rehabilitación permitiendo al paciente el control de ortesis robóticas controladas directamente desde señales del cerebro o a través del envío de Estimulación Eléctrica Funcional(FES) directamente asociada con la activación del Sistema Nervioso Central, lo cual es muy importante para que pueda darse una rehabilitación exitosa del paciente.

Nuestro trabajo de tesis consiste en un problema particular de decodificación motora: La detección del tipo de agarre realizado en un movimiento funcional de arranque, agarre del objeto y manipulación de este; a partir de el registro de la actividad cerebral con Electroencefalografía (EEG). Hay dos objetivos principales en esta tesis, el primero consiste en un análisis del EEG para encontrar correlatos neuronales asociados al movimiento de agarre, específicamente se busca encontrar y estudiar la dinámica de Potenciales Corticales Relacionados al Movimiento(MRCP), que son correlatos neurales asociados a actividades motoras . El segundo objetivo consiste en la descodificación de dos tipos de agarre (agarre de fuerza y agarre precisión) a partir de señales cerebrales utilizando MRCPs.

Para esto se diseñó un protocolo experimental, se registraron a 10 sujetos sanos y se evaluaron fuera de línea los registros. Tanto para el análisis del EEG como para la descodificación se evaluaron y utilizaron diversas técnicas de procesamiento de señales y de aprendizaje automático.

Nuestros resultados obtenidos fueron los siguientes: En lo que respecta al análisis del EEG, se encontraron Potenciales Corticales Relacionados al Movimiento(MRCP) durante los movimientos funcionales de agarre. A más de esto, se realizaron varias observaciones sobre la evolución temporal de los MRCP en tareas funcionales de agarre. Con respecto al segundo objetivo, por medio de algoritmos de clasificación como Análisis Discriminante Lineal y Máquinas de Soporte Vectorial con función de base radial como kernel, se logró descodificar entre el descanso y la acción de agarre con una exactitud de 76.74%. Así también se logró la descodificación entre un agarre de fuerza y uno de precisión con una exactitud de 64.89 %.

List of Abbreviations

AP	Action potential
BCI	Brain Computer interface
BOLD	Blood oxygenation level dependent
CNS	Central nervous system
CSP	Common spatial patterns
ECoG	Electrocorticogram, electrocorticography
EEG	Electroencephalogram, electroencephalography
EMG	Electromyogram, electromyography
EOG	Electrooculogram
EP	Evoked potential
ERD	Event-related desynchronization
ERP	Event-related potential
ERS	Event-related synchronization
FES	Functional electrical stimulation
fMRI	Functional magnetic resonance imaging
fNIR	Functional near infrared
ICA	Independent component analysis
LDA	Linear discriminant analysis
MI	Motor Imagery
MRCP	Movement Related Cortical Potential
PCA	Principal Component Analysis
SAO	Somatosensory Attentional Orientation
SCP	Slow Cortical Potential
SMR	Sensory Motor Rhythm
SNR	Signal to Noise Ratio
SVM	Support Vector Machine

Contents

Chapter 1

Introduction

1.1 Brain Computer Interfaces for Neurorehabilitation

Some neurological diseases like stroke or spinal cord injury cause a decrease of motor capacities. Patients diminish their mobility and manipulation capacities with a consequent affectation in their daily life activities such as cleaning, feeding or dressing; as a consequence, these individuals have severely limited their autonomy with a negative impact in their participation in society meaning a decreasing quality of life as well.
One of the leading causes of such impairments is stroke, which in some developed countries can be the third leading cause of death, after heart disease and all forms of cancer [1]. Furthermore, for most of the countries considered by World Health Organization, stroke incidence varies between $50/100\ 000$ and $150/100\ 000$ population per year [2], revealing a growing world-wide burden of stroke. This high rate of incidence is increasing due to aging society although better survival rates thanks to medical advances. This has increased the impact on society which takes a toll on many levels affecting the person, his close relatives and the health services. Rehabilitation has become of utmost importance and is the general context of this thesis.
The rehabilitation process for neurological diseases deriving in motor decline works as follows: cortical or subcortical lesions disrupt the connection between peripheral muscles and the sensorimotor cortex; however, a concurrent activation of sensory feedback loops and the primary motor cortex may reinforce those dormant cortical connections through Hebbian plasticity mechanisms. It means that recovery of sensory and motor capacities may be possible over time.
Current rehabilitation of these patients is done by passive repetition of exercises with the affected limb, which gradually gains speed, strength and precision in their movements.
Since complete recovery is not always achieved by classic rehabilitation techniques, there is an interest in pursuing other alternative approaches that can provide a gain in the functional recovery of patients. They include electrical stimulation to increase cortical excitability during training, drugs to optimise molecular mechanisms for learning, stem cells therapies and practice with robotic devices or in a virtual environment. A great advantage of the use of robots in rehabilitation tasks is the on-line evaluation of the work during the routines, as well as guide patient movements.
However, in order to succeed, it is important to keep the user active and in the loop so that brain plasticity may be induced by correlating cortical activity with movements per-

formed. Advances in neuroscience and brain imaging technologies enable nowadays one promising solution that improve the former scenarios end even goes beyond due to implicate active participation of Central Nervous System (CNS) in rehabilitation; this solution is provided by Brain Computer Interfaces (BCI).
In this thesis we are going to focus on the use of this type of neuro-robot or exo-skeletons controlled by brain commands in such a way that CNS is involved.

BCIs to involve the CNS in neuro-rehabilitation

A Brain-Computer Interface (BCI) is a system that provides the brain with a new, non-muscular communication and control channel[6]. In others words, user's intent goes directly from brain to an external device, bypassing conventional channels of communication.
Brain-computer interface (BCI) systems allow the use of brain signals, both for assistance and rehabilitation goals, by detecting primary motor cortex activation (motor imagery or intention to move) in users and then, provide them with a matched sensory feedback (i.e., through functional electrical stimulation (FES), virtual reality environments, or robotic systems)(see Fig. 1.1).

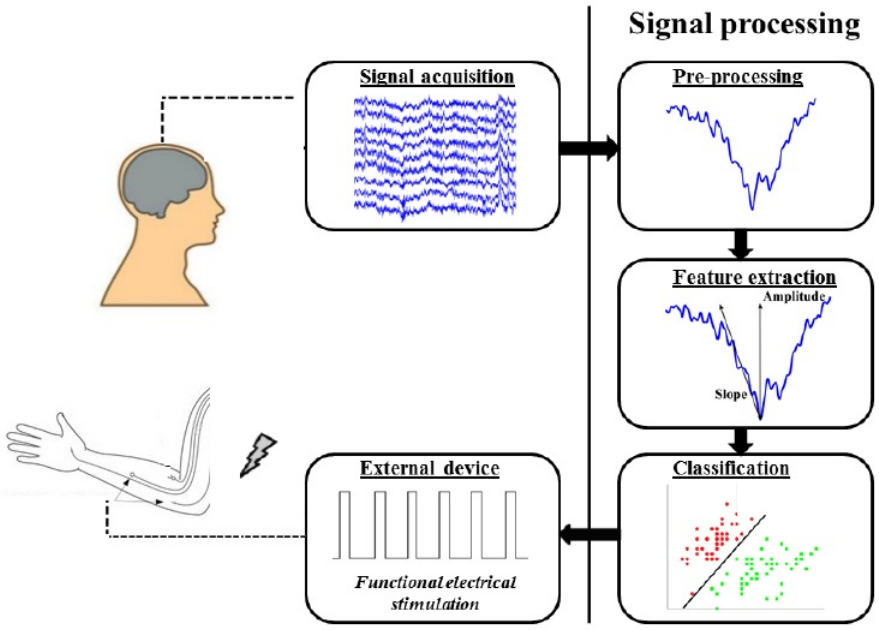

Figure 1.1: General scheme of a Brain Computer Interface for rehabilitation purposes. In this figure, the output from classifier drives a feedback sent to user consisting of FES (but it might be commands to drive a robotic device)

Therefore, a BCI system with application in neurorehabilitation, induce activity-dependent plasticity by making the user pay close attention to a task requiring the activation or deactivation of specific brain areas [4] and then correlate, in a specific timing, this motor cortex activation with feedback.
On the other hand, when it is not possible a motor recovery by rehabilitation methods; a BCI can also provide motor substitution to handicapped by allow user to move their

paralysed limb with an orthotic device or even a prostheses (for amputees) commanded from high-level brain commands.
Until this point, we have introduce the rehabilitation context for neurological diseases implying loss of motor capabilities, and we have stated how a BCI is an utmost and promising solution scenario for neurorehabilitation. Technical details of how a BCI works are found in next chapter. Additionally we just mention that there are many other applications of BCI such as communication and control, training and education, games and entertainment and some others. However, this thesis work focus in motor brain computer interfaces with application in neurorehabilitation.

1.2 Motor Brain Computer Interfaces: state-of-the-art and challenges

In a nutshell, a BCI works as follows: It records brain activity using some of the existing neuroimaging technologies. Then, the BCI detects and classifies, into the ongoing brain signals, specific patterns of activity associated with specific tasks or events; when these tasks/events are motor actions we refer to the BCI as a motor BCI. Additionally, a mental strategy (or approach) need to be determined in a BCI in order to induce brain patterns to be further decoded. In the last years, there have been promising results in in motor BCIs, though there are still current challenges to export BCI from lab to real life applications. In this section we are going to describe the state of the art of motor BCIs oriented towards rehabilitation.

1.2.1 Motor imagery

One of the most common mental strategy in motor BCI, oriented to neurorehabilitation, is Motor Imagery (MI). MI is based on detectable effects on certain brain signals produced by particular imagined tasks like imagination of repetitive opening and closing hand, and imagination of feet movements. MI based BCI, exploit sensorimotor rhythms (SMR) associated with the imagination of movements. It is well know that these tasks induce a power increase or decrease of EEG amplitudes in certain frequency bands.
MI can be performed either obeying a cue triggered by the BCI protocol (in that case the protocol is called cue-based) or performed at the time desired by user (self-paced protocol). Figure 1.2 illustrate a motor imagery protocol developed in the so called Graz-BCI paradigm.

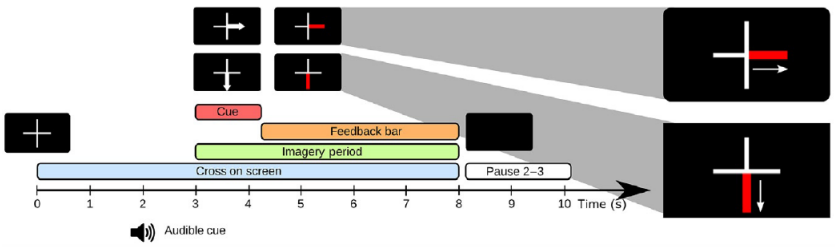

Figure 1.2: Protocol timming in the Graz-BCI based on MI

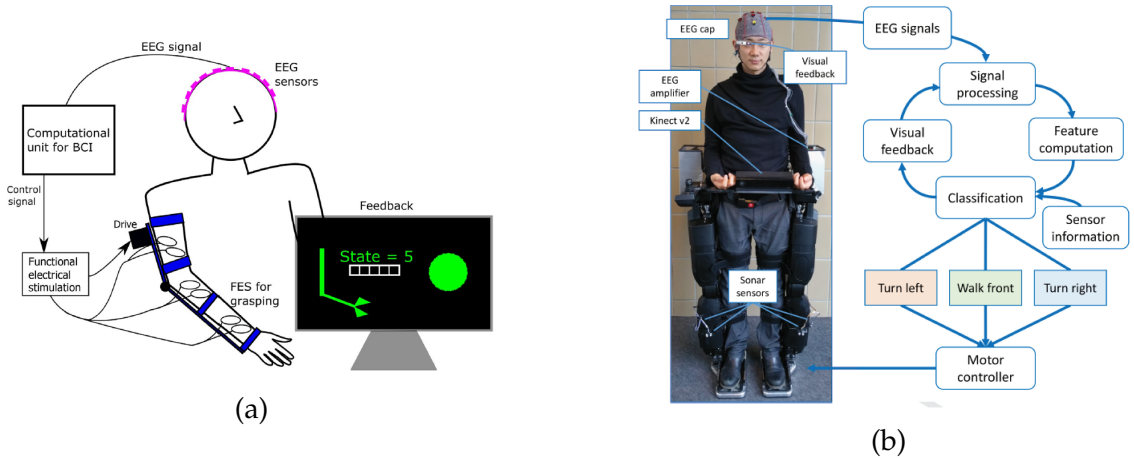

Figure 1.3: **(a)** Schematic of a hybrid BCI for controlling an upper extremity neuroprosthesis (Rohm et al., 2013). **(b)** Rex Exoskeleton controlled through cascaded ERD Classifiers(K. Lee et al., 2016)

This type of BCIs have been used to control of extremity neuroprosthesis [7] or even an exoskeleton for lower limbs [8] (see Fig.1.3).

Additionally, some other paradigms related to motor imagery like Somatosensory Attentional Orientation (SAO) have been explored and included in hybrid BCI systems [12]. One of the main drawback in the classic MI-BCI approach is the long time for training period. Some advances in MI-BCIs include implementation of coadaptive approaches to reduce the training period required in these BCI systems[9] [10] [11].

Despite all the achievements in MI based BCIs in the previous years, control of prostheses by motor imagery lacks of natural control since movement imaginations do not necessarily correspond to the neuroprosthesis movements. Moreover, latency of detection is in the order of seconds, which is not desired for successfully rehabilitation process. Therefore, to achieved a natural and intuitive control of neuroprostheses, is needed a framework that incorporate complex movement intention decoding such as decoding of arm kinematics movements, decoding goal movement, and grasp type decoding [13].

1.2.2 Decoding of functional movements

Beyond decoding imagination of general movement of limbs, current state of the art in motor decoding focus on decoding complex movements from EEG, since there exists neural signatures present in EEG when functional movements are performed. These neural signatures, or neural correlates, of motor activity are Sensorimotor rhythms (SMR) and Movement Related Cortical Potential (MRCP) which are further explain in next chapter. Thus, the current framework of complex movements decoded in BCI systems for neurorehabilitation comprise gait, upper limb kinematics, goal movements and grasping. These systems, oriented to varied applications, are reviewed next.

Gait

Neuroimaging studies provide evidence of cortical involvement immediately before and during gait and during gait-related behaviors such as stepping in place. Diverse studies have used neural correlates of lower limbs movements to classify gait intent from another movement plan(point intent)or from standing in place [36]. Intention to walk have been succesfully detected even in stroke patients [34]. Moreover, these findings has lead to develop BCI systems to control an ambulatory exoskeleton without any weight or balance support for gait rehabilitation of incomplete spinal cord injury(SCI) patients[37] (see Fig.1.4). Continuous decoder has also achieved high level decodig performance without session-to-session recalibration [38].

Figure 1.4: Control of an ambulatory exoskeleton with a Brain Computer Interface for spinal cord injury gait rehabilitation [37]

Goal-directed movement intention

In a reach-and-touch task, it is of great interest for research in both neuroimaging and BCI, explore if there exits discriminable differences in brain activity between goal-directed and non-goal-directed movements. Diverse studies [27] [27] have shown that goal-directed movements differ from non-goal-directed movements with the same kinematics. These differences are found in low-frequency time-domain EEG signals and they may be employed to improve movement intention classification accuracies.

Center-out reaching movement

Another functional movement that has attracted attention, and contribute to the framework of kinematics motor decoding is center-out reaching task. Experimental protocols for these studies consists in performing a center-out movement in front of a screen showing target locations [29] [30]. Discrete classification decode movement targets with significant classification accuracy. However, the principal aim is to decode the kinematics performed. Results suggest that classification of reached targets from decoding approaches may be a more suitable real-time methodology than a direct decoding of hand position.

Kinematic decoding

One of the most pursued objectives in motor decoding is decode movement kinematics from EEG movements correlates. Decoding information is extracted from low frequency bands. Linear regression methods are used to decode kinematics, validated through correlation techniques. In previous years, diverse studies have been performed to decode 2D/3D limb kinematics from low-frequency EEG [30] [31] [32] . Nevertheless, the use of a linear regression model implies that the relevant component of the signal used for decoding (EEG) has to be in the same frequency range as the signal to be decoded (velocity profiles); furthermore, the use of a correlation to evaluate the decoding could lead to overly-optimistic results [33].

Grasp decoding

Grasp action has been investigated in previous years by diverse imaging studies. However, there is a missing of studies that take advantage of the temporary resolution of the EEG and validate results obtained with other neuroimaging techniques. Besides, decoding grasp may be of great importance in BCI domain; on the one hand, for strengthening current framework of motor decoding to achieve a natural way of neuroprostheses control; on the other hand, it may enhancing neurorehabilitation through BCI systems.

1.3 A particular functional movement: Grasp action

Grasp is one of the most important motor skills in humans. It is well know that hand anatomy with opposable thumb, so distinctive in humans and primates, allow performing power grip and precision grip. These two kind of grips is a general taxonomy from functional and a phylogenetic perspective first suggested by Napier [49]. Power grip is a palmar opposition grasp in which all digits are flexed around the object to provide high stability. The precision grip is performed for the manipulation of small objects with the tips of the thumb and fingers. It requires for stability independent finger movements that involve fine control of the directions and magnitudes of fingertip forces.

Our interaction with the objects of our environment is possible thanks to these sophisticated motor mechanisms of grip and derivatives thereof. We may even presume that the vast majority of our activities of daily living consist of functional movements that end in a gripping action. The functional movement that comprises reaching an object with the hand and grasping it, is called prehension. This human ability has also motivated robotics and biomechanics, leading to emulate human grasp to make robot devices become more accurate in the tasks they perform.

1.3.1 Neuroscience of grasp

In regards to neuroscience, grasp in humans and primates have been extensively investigated. These studies aim to integrate information from various domains to ascertain which neural circuits underlie grasping [50]. Previous monkey neurophysiological and human neuroimaging studies demonstrated that planning and execution from reaching

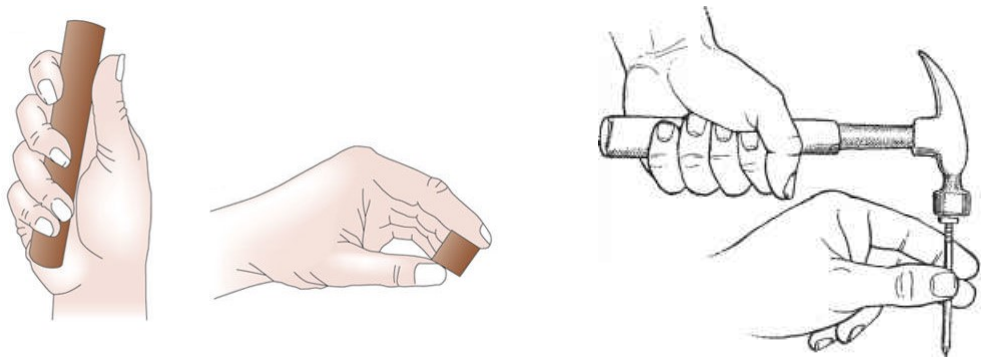

(a) (b)

Figure 1.5: **(a)** Power grip (left) and precision grip (right). **(b)** Power grip and precision grip exemplified in a common task

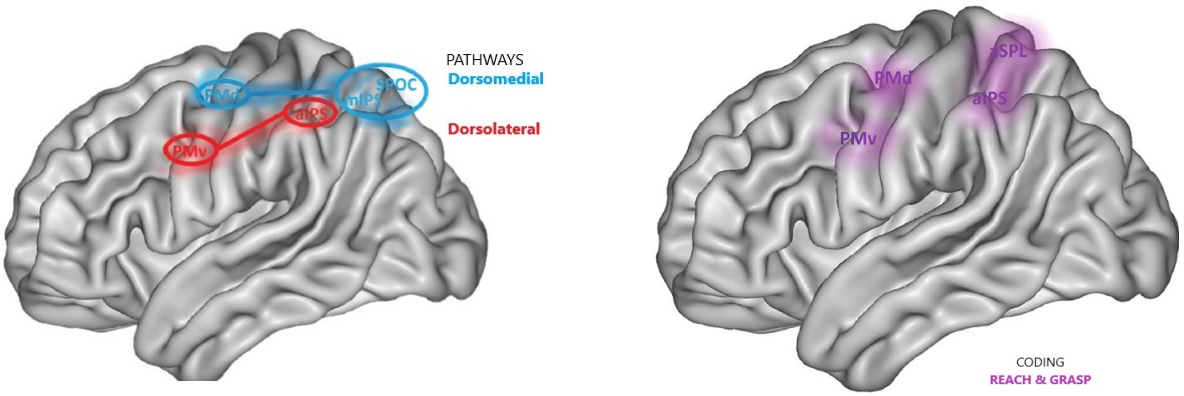

(a) (b)

Figure 1.6: **(a) Pathways (circuits) identified in prehension movement**. Dorsolateral circuit link ventral premotor cortex(PMv) and anterior intraparietal sulcus(aIPS). Dorsomedial circuit comprise dorsal premotor cortex(PMd) connected to the superior parietal occipital cortex(SPOC), and medial intraparietal sulcus(mIPS). **(b) Brain areas in premotor cortex involved in coding both, reaching and grasp.** Same regions previous mentioned and anterior superior parietal (aSPL)

to grasping, is encoded within specific neural substrates: the prehension network [50].

In monkeys, this network comprises dorsomedial and dorsolateral pathways connecting regions within the posterior parietal cortex (PPC) with regions of the frontal cortex possessing. Coding of reaching and grasping occur in different areas within PPC according to diverse studies [55] [56]. In past years, a similar model was conceived for humans. More recently, diverse studies have found that there are two circuits dorsomedial and dorsolateral involving in prehension in humans. However, there are no dissociative brain regions coding the stage of reach and grasp in a functional movement [57](see fig.1.6).

Up to now, it has been defined where grasping(i.e.,grip information)is coded and which regions are causally involved in its processing. However, it is still missing information about when and where grasping is integrated with reaching (i.e.,transport information). Most of the studies have been carried with neuroimaging technologies with good

spatial resolution but poor temporal resolution. Some recent EEG studies suggest that the two circuits interact during prehension coding and that the dorsolateral pathway could drive processing within the dorsomedial one [51].

On the other hand, regarding force and precision grips, an fMRI study [53] indicates that power grip is associated predominately with contralateral left-sided activity, whereas the precision-grip task involved extensive activations in both hemispheres. Thus, those findings indicate that in addition to the primary motor cortex, premotor and parietal areas are important for control of fingertip forces during precision grip. Moreover, the ipsilateral hemisphere appears to be strongly engaged in the control of precision-grip tasks performed with the right hand. There is also missing information about these two kinds of grips provided by imaging techniques focus on high temporal resolution.

1.3.2 Decoding of grasp types from EEG

In the previous section we briefly mentioned current neuroscience results related to grasp and reaching as a functional movement. Regarding to decoding grasp types from cortical signals, there are few studies addressing this topic [60][61].
Extraction of neural correlates of grasping and decoding of grasping types from non invasive technologies is of great interest not only for neuroscience research but also for Brain Computer Interface community.
Current BCI systems for rehabilitation and motor substitution, restore some degree of functional ability, but fail to approach the dexterity of the natural hand, particularly for grasping movements. Therefore, decoding grasp types from non invasive techniques such as EEG, has become a matter of great importance in the last years. In this section we review the state of the art of grasping decoding from EEG oriented to Brain Computer interfaces.

Randazzo et al. present in [64] a technique that exploits Movement Related Cortical Potentials (MRCP) as EEG neural correlates to decode grasping during reaching movements. Results obtained with four subjects show the existence of Slow Cortical Potentials (SCP) prior to the execution of grasping movements and how they can be used to classify, with accuracy rates greater than 70% across all subjects, the intention to grasp.
In a later study, Inaki et. al. [63] found that the two grasping types were significantly different ($p<0.01$, Bonferroni corrected t-tests). To discriminate between the two grasping types, they use contra-lateral motor channels using the activity prior to the grasping onset. Grasping types were detected with an accuracy of $75.90 \pm 5.02\%$ on average across subjects.

Schwarz et al. in [65] , perform an experiment over fifteen healthy participants, in a cue guided paradigm subjects were instructed to perform 3 different reach-grasp-hold tasks on 3 different objects: palmar grasp (cylinder), pincer grasp (needle) and key grasp (key). They confirmed that grasp versus grasp classification in the low-frequency time-domain is possible. Fourteen out of 15 participants scored significantly better than chance in at least one combination, whereas 8 participants performance topped 70%.

Agashe et al. performed in [59] kinematic decoding in reach and grasp movements. In that experiment, five different objects need to be grasped. They also performed a discrete

classification to discriminate between five grasp types. They reported grasp classification peaked after movement onset.

1.4 Thesis overview

Regarding to this thesis work, we first took Motor Imagery (MI) approach as a starting point for this thesis work during our intern at the National Rehabilitation Institute (INR) in Mexico City. Research group at INR developed a MI-based BCI for rehabilitation therapies. That BCI detects, in a cue based environment, motor imagery tasks performed by stroke patients and send a feedback of successfully detection through a robotic hand orthoses.
Despite the promising results obtained by MI BCIs, there are two main drawbacks in MI approach. First, they solely rely on detecting the limb (usually both feet, right hand, left hand) subjected to the movement imagination (MI) resulting in a low number of classes, thus natural control cannot be achieve. On the other hand, the delay between the movement intention detection and the actual user's intention is in the order of seconds, which is not short enough for the Hebbian principle to be applied. A short temporal gap between the user's intention and the feedback provided (e.g. electrical stimulation; robotic devices control) is fundamental to promote motor recovery at the cortical level, inducing neural plasticity.

For this thesis work, we also establish a partnership with BitBrain Technologies ®, a neurotechnology enterprise located in Zaragoza, Spain. During the intern at BitBrain, we move away from motor imagery approach to decide investigate neural correlates of a specific movement, that is neural correlates of grasping.
Finding neural correlates of grasping in EEG recording, and decoding the type of grasp performed from the ongoing signals; is of great importance for research on neuroimaging as well as for Brain Computer interfaces oriented to neurorehabilitation.
Regarding to BCI for neurorehabilitation, a BCI for grasping might use high-level commands to activate several muscle groups in coordination by FES, or controlling a hand orthoses with many degrees of freedom in a natural way.

This thesis work approaches the context of a BCI for rehabilitation purposes with the particular goal of decoding grasp type from EEG. This thesis comprehends from the designing of an experimental approach, EEG analysis concerning to neural correlates of grasping action, until decoding of grasp types through a classification stage.

Preliminary Questions

The following preliminary questions comprised the depart point of our research:

Neural correlates in a grasp action The first question we posed in our study was about existence of neural correlates of grasping into EEG. Since MRCP have been considered as neural correlates in motor actions, we wanted to ascertain MRCP during grasp actions; that is, *how is the nature of MRCP during grasp actions?* Furthermore, since grasp functional

movement comprises various movements stages, *how many typical MRCP morphologies can be seen in the time course of the functional movement?*

Pipeline proposal *Which processing techniques should constitute a pipeline leading to grasp decode from EEG?*

Time-lock signals Typical deflection and point of maximum negativity in MRCP occurs in a specific time with respect to a movement onset. Since a grasp functional movement comprises various movements stages, *To which of them is MRCP time-locked?* There is a difference among studies concerning to the moment the signals are time-locked to. Thus we answered that question through our experimental setup.

Decoding grasp types Assuming the existence of neural correlates of grasping, *are there discriminative differences between force grip and precision grip? How are these differences encoded? latency, amplitude or some other MRCP feature?* Then, if we may capture these encoded differences in a feature vector, *are classification results above chance level to ensure BCI applications?*

Thesis structure

The thesis structure is as follows: This first chapter called Introduction, presents the general context of Motor Brain Computer Interfaces oriented to neurorehabilitation, as well as the state of the art concerning to grasp decoding from EEG; it ends with the thesis overview. Second chapter introduce a general framework for motor BCI, here we present theoretical background of some methods applied in this thesis. Methodology is the third chapter, it comprises all stages followed for both, an EEG analysis looking for neural correlates of grasping, and a decoding of grasp types from EEG signals. Results of each of the previous stages performed are introduced in fourth chapter. Conclusions and discussion about the results obtained comprise the last chapter as well as future works.

1.5 Objectives

Main Objectives

We introduce here the main objectives followed through this thesis work.

- **Finding neural correlates of grasping as a functional movement**
- **Decode type of grip performed from EEG signals**
- **Contribution to the motor decoding framework towards Brain Computer Interfaces for rehabilitation purposes**

Secondary Objectives

There are some secondary objectives deriving from principal goals. These are:

- **Revision and assembling of the state-of-the-art concerning to motor decoding from EEG**
- **Design of experimental protocol**
- **Data recording**
- **Implementation and validation of preprocessing techniques**
- **EEG analysis oriented to motor decoding**
- **Grasp actions decoding using MRCP features**

Chapter 2

Brain Computer Interfaces

This chapter introduce general framework about Brain Computer Interfaces regarding this thesis work. The general BCI architecture comprises the following general stages of brain signal processing: signal acquisition, signal preprocessing, feature extraction and classification. Theoretical background of each one of these stages is explained through this chapter.

2.1 Measuring Brain Activity

The first stage in a Brain Computer Interface consists in recording brain activity. Diverse BCI technologies have been developed using different acquisition schemes. There are two general classes of brain recording technologies: invasive technologies, in which sensors are implanted directly on or in the brain, and non-invasive technologies, which measure brain activity using external sensors [14].
Among the invasive acquisition technologies, we can mention Electrocorticography (ECoG) [15] [16] , which consists of electrodes placed on the surface of the cortex. Intracortical recording is another invasive technology [17], here electrodes penetrate brain tissue allowing recording the neural activity of a single brain cell or small assemblies of brain cells. Invasive recording techniques provide high temporal and spatial resolution, besides artifacts are less problematic. Despite all these advantages, invasive recordings are impractical as they require surgery, implying financial and ethical issues. Furthermore, once implanted, these technologies cannot be moved to measure different regions of the brain and signals loss stability over time.

Another alternative in BCIs, is the use of non-invasive methods. Magnetoencephalography (MEG) [18] records magnetic fields associated with brain activity. Functional Magnetic Resonance Imaging (fMRI) [19] and Near Infrared Spectroscopy (NIRS) [20] are based in the fact that for neuron communication, more oxygen and glucose is needed causing an increase in blood flow. The former technique measures small changes in the blood oxygenation level-dependent (BOLD) signals while the later technique measures optical properties caused by these differences in oxygen levels of the blood. These non-invasive techniques above mentioned are quite expensive, require large devices and have low time resolution (>2–5 seconds); these drawbacks make them impractical for typical BCI applications. However, as they provide high spatial resolution (<1 cm), general models obtained by these techniques are used in brain activity source localization algorithms.

Electroencephalography (EEG) is the most used non-invasive technology in BCI research; due to its lower cost, greater applicability, high time resolution and less time to place the scalp electrodes. As we use this acquisition technique in this thesis, next subsection is dedicated to widely explain EEG as neuroimaging technique for BCI.

2.1.1 Signal acquisition with Electroencephalography

Electroencephalography (EEG) uses electrodes placed directly on the scalp to measure the electrical potentials (5–100 μV) generated by brain activity. The acquisition system measures and amplifies the potential difference from all electrodes (channels) referred to one common electrode, typically called reference and labeled Ref. An additional "ground" electrode, labeled Gnd, is required in amplifiers to improve signal quality.

EEG electrode naming and placement

The standard naming and positioning scheme for EEG applications is called the 10–20 international system [21]. The "10" and "20" refer to the fact that any electrode is either 10% or 20% of some distances from another. In this system, each electrode is named with letters and a number according to its position (region and side) over the scalp. The first letters in the label, indicate that the electrode is within a certain brain region (lobe) such as Fp – pre-frontal, F – frontal, C – central, P – parietal, O – occipital, T – temporal (see Fig. 2.2). A number is set next to the letter, odd numbers indicate left hemisphere and even numbers denote right hemisphere placement. Numbers in electrode's labels are in ascending order indicating how far away from the longitudinal line which set at the center(z).
Electrodes are placed on imaginary arcs delineated over the scalp. These lines are traced considering reference points on the skull: Nasion (Ns), Inion (In), and Left and Right Pre-Auricular points (PAL and PAR, respectively). The intersection of the longitudinal (Ns–In) and lateral (PAL–PAR) diagonals is named the Vertex, Cz electrode is placed at this point (see Fig. 2.1).

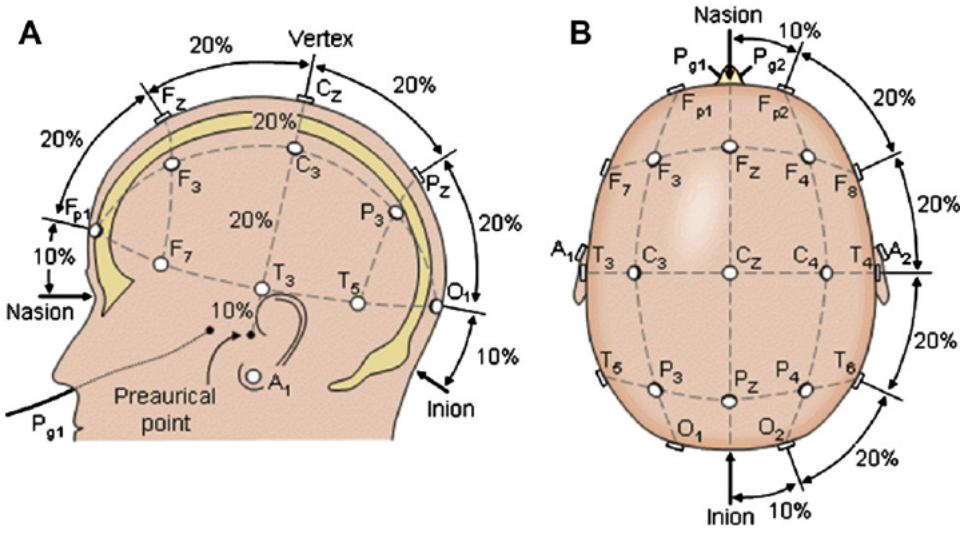

Figure 2.1: Electrodes on the original 10–20 scheme

Acquisition with an EEG cap

Mounting EEG electrodes is vital in order to acquire good signals. Most of acquisition systems uses elastics caps that already have an arrangement of electrodes in a standard fixed position. As it is very important in a EEG register knowing how to placed this caps, we mention next a technical proposal mentioned in [22].

- Mark the vertex on the subject's scalp using a felt-tip pen or some other similar method. Begin by locating the nasion and inion on the subject as indicated in panel A of 2.1 Using a tape measure, find the distance between these two locations. The point half-way between the two points is the vertex. Make a mark at that point for later reference. (Other 10–20 points could be located in a similar manner)
- Mark scalp positions for Fpz and Oz. The Fpz position is above the nasion 10of the distance from the nasion to the inion. The Oz position is above the inion the same distance.
- Identify the Cz electrode on the EEG cap and place the cap to position the Cz electrode on the vertex.
- Keeping Cz fixed, slide the cap onto the head.
- While ensuring that Cz does not shift, adjust the cap such that the Fz–Cz–Pz line is on the midline; Fp1–Fp2 line is horizontal, and at the level of the Fpz mark; the O1–O2 line is horizontal, and at the level of the Oz mark.
- You can now fix Ref and Gnd electrodes. These electrodes are attached in one of a few typical configurations. One common configuration is to attach the Ref electrode to one earlobe, and the Gnd electrode to the mastoid on the same side of the head. Another possible configuration is to attach Ref to one mastoid and Gnd to the other mastoid. This choice is influenced by the used cap technology, which may have separate electrodes outside the cap for reference and ground, or may have these electrodes embedded in the cap directly.

2.2 Brain Signals for motor decoding

A motor event implies neuronal changes in brain structures. There exist two main cortical patterns extracted from EEG that reflects a motor activity. They are Event-related Potentials (ERPs) and Cortical Oscillations. In these brain signals, there exist neural correlates directly associated with user's motor intention. The main goal of a motor BCI system is to detect and decode user intention through these neural correlates. Since this thesis focus on motor applications of BCI, we describe next some types of brain signals that are more important for motor decoding.

2.2.1 Sensorimotor rhythms (SMR)

Sensorimotor rhythms (SMR) refer to cortical oscillations in brain activity recorded more exactly from somatosensory and motor areas (see Fig.2.2). Brain oscillations are typically categorized according to specific frequency bands which are named after Greek letters (see Table 2.1).

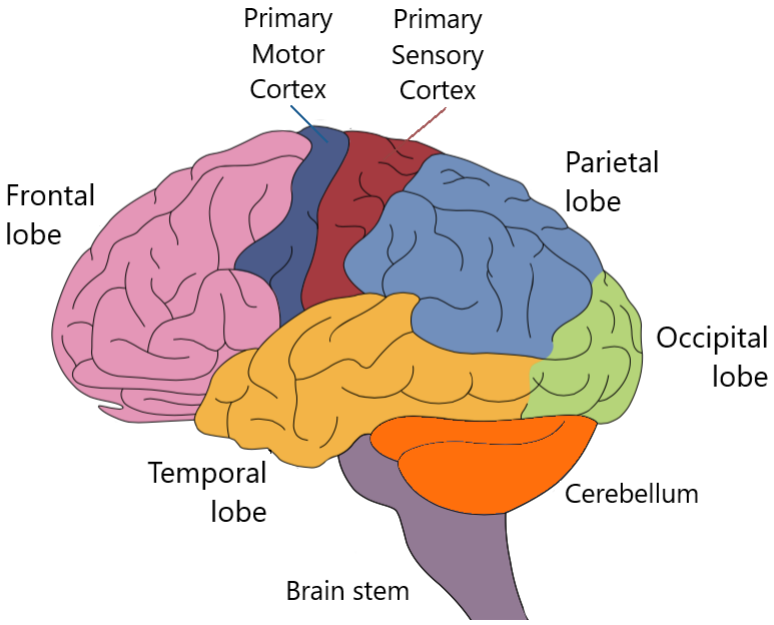

Figure 2.2: Brain regions.

Brain Waves	Frequency
Delta	1-4 Hz
Theta	4-7 Hz
Alpha	8-13 H
Betha	12-25 Hz
Gamma	>25 Hz

Table 2.1: EEG Frequency bands.

Modulation of brain oscillations makes reference to detectable changes of EEG rhythms induced by self-controlled brain activities. Modulation of brain rhythms can be sorted into the following three classes: power modulation, frequency modulation, and phase modulation [43]. Many current BCI systems are designed based on the modulation of brain rhythms.

For a signal $s(t)$, its analytical signal $z(t)$ is a complex function defined as:

$$z(t) = s(t) + j\hat{s}(t) = A(t)e^{j\phi(t)} \tag{2.1}$$

Where $\hat{s}(t)$ is the Hilbert transform of $s(t)$, $A(t)$ is the envelope of the signal, and $\phi(t)$ is the instantaneous phase. Changes of the modulated brain rhythms can be reflected by $A(t)$ or $\phi(t)$ [43].

Power modulation The event-related increase and decrease of power change, of brain rhythms in a specific frequency band, is well known as Event-Related Synchronization and Desynchronization (ERD/ERS) respectively. ERD/ERS patterns can be volitionally produced by motor activity, even by motor imagery (imagination of movement without actually performing the movement). This last statement has been exploited by BCIs based

on motor imagery that was the most common motor BCI system in previous years
Alpha activity recorded from sensorimotor areas is also called Mu (μ) activity. The EEG frequency bands that are most used for extraction of ERD/S patterns are μ and β. There are also some studies suggesting that movement related activity can be also detected in the high gamma range of the human EEG [42]. We did not test this approach since we were mainly focused in Slow Cortical Potential that are explained next.

2.2.2 Slow Cortical Potentials (SCP)

Slow Cortical Potentials (SCP) are categorized as Event-related Potentials (ERPs). Brain processing of a sensory stimulus or another event can produce a time-locked series of positive-negative deflections in the EEG. These ERP components are distinguished by their scalp locations and latencies. Visual Evoked Potential (VEP) and P300, are some others ERPs. Together with SMR signals, they were used in the past years in BCI systems for control and communication oriented to rehabilitation. However, nowadays research is focused in neural correlates directly associated with movements, which is the case of SCP. Respecting to SCP, they are slow voltage changes generated in cortex (occuring in delta band) and have latencies up to several seconds or even minutes. SCP reflect response-oriented brain activity and self-initiated movements. In normal brain function, negative SCPs accompany mental preparation, while positive SCPs probably accompany mental inhibition. Negative and positive SCPs probably reflect an increase and decrease, respectively, in excitation of cortical neurons [5].
A particular type of SCP is Movement Related Cortical Potential (MRCP), reported first by Kornhuber and Deecke(1964) [44]. MRCP is a signal time-locked to movement onset, identified by averaging time-lock epochs. The MRCP is characterized by a slow negative deflection before movement execution (ME), imagination, and attempted ME; reaching the maximum negativity near the onset, which is followed by a positive rebound before returning to the baseline level. Technically speaking, the MRCP comprises four principal components (see Fig. 3.14): the Bereitschaftspotential (BP) or Readiness Potential (RP), Pre-Motion Positivity (PMP) or BP2, Motor Potential (MP) and reafferente potentiale or Movement-Monitoring Potential (MMP); the first three occur prior to movement onset while the last one after movement onset [45].

One of the advantages of considering MRCPs as neural correlates of movement is that, for upper limb movements, the MRCP magnitude and slope are known to be modulated by movement-related parameters, like speed [24] and force [25], as well as allowing discriminate analytic movements of the upper limb [26]. MRCP are also considered as neural correlates of gait [34] [35]. Furthermore, MRCPs has been shown to have relatively short latencies, reducing the time between the actual intention and the system response.
Event Related desynchronization/synchronization (ERD/ERS) of sensorimotor rhythms (SMR) and the Movement-Related Cortical Potentials (MRCP) are typical cortical signatures of motor tasks.

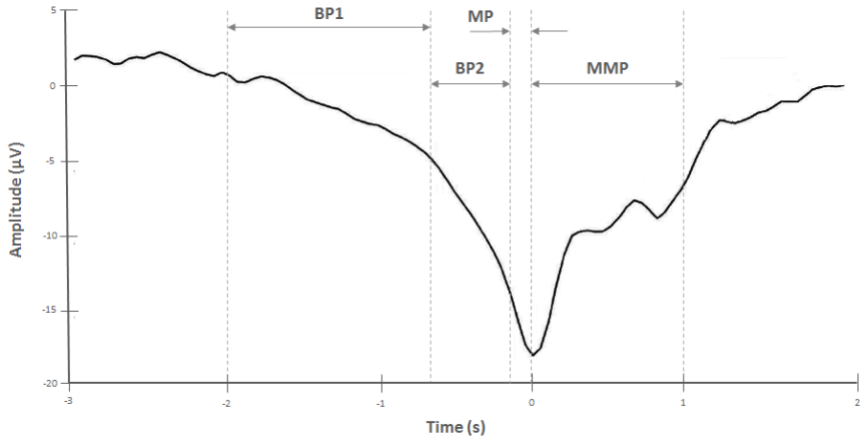

Figure 2.3: MRCP signal and their identifiable components. (Different terminologies have been proposed for MRCP components)

2.3 Signal Preprocessing

After EEG signals (related to a specific task or events) have been recorded; the goal of the BCI system is decode the task or events from those signals. In order to achieve an accurate decoding, it is often necessary to enhance spatial resolution and signal to noise ratio. That is, improve Central Nervous System (CNS) activity signals and detect and reduce non-CNS activity; such as Electromyography (EMG) activity and Electroculography (EOC). In brief, in this stage called preprocessing, the aim is removing noise and artifacts, enhance Signal to Noise Ratio (SNR), and reduce spatial blurring.
Preprocessing methods include spatial and temporal filtering techniques, signal averaging, and single-trial recognition. This section describe with more detail some of these methods. First, typical artifacts in EEG are mentioned. Then, temporal filtering is introduced and spatial filtering methods are described.

2.3.1 Typical EEG artifacts

EEG records electrical activity on the scalp. Ideally EEG looks for record brain activity from cerebral cortex, however some others electrical activities not related to brain activity are records as well, these undesired electrical elements are called artifacts. Artifacts may be divided into physiologic and extraphysiologic artifacts. The former are generated from human body (e.g. muscles, eyes, etcetera). Extraphysiologic artifacts arise from outside the body (i.e., equipment, environment). We mention next some common physiological artifacts that must be dealing with in a preprocessing stage.

Muscular artifacts

It is well-known that the power spectrum of contracting striated muscle, measured with surface electromyography (sEMG), shows a bandwidth of 20–300 Hz and that most of the power is in the lower end of this frequency range. Since the frequency distribution of

EMG signals is very broad, they have a profound effect on amplitudes in typical mu/beta frequency ranges. The peak frequency of the masseter muscle, involved in chewing, is around 50–60 Hz, whereas for frontalis, the muscle which controls wrinkling of the brow, it is 30–40 Hz [23].
EMG artifacts are usually overcome by applying low-pass filters. However, if high-frequency neural activity is analyzed (such as gamma-frequency band), it overlaps entirely with the spectral bandwidth of muscle activity.

Eyes related artifacts

Eye blink. When a person blinks, an artifact is induced in EEG record. It is caused by friction between lid and cornea. This movement results in charge separation, with a dominantly dipolar charge distribution, and the dipole moment pointing in up-down-direction [22]. In the EEG, this effect is recorded as a positive peak that lasts a few tenths of a second, is most prominent in the frontopolar region, but affects all the electrodes of the montage, attenuating with distance from the front (Fig. 2.4).

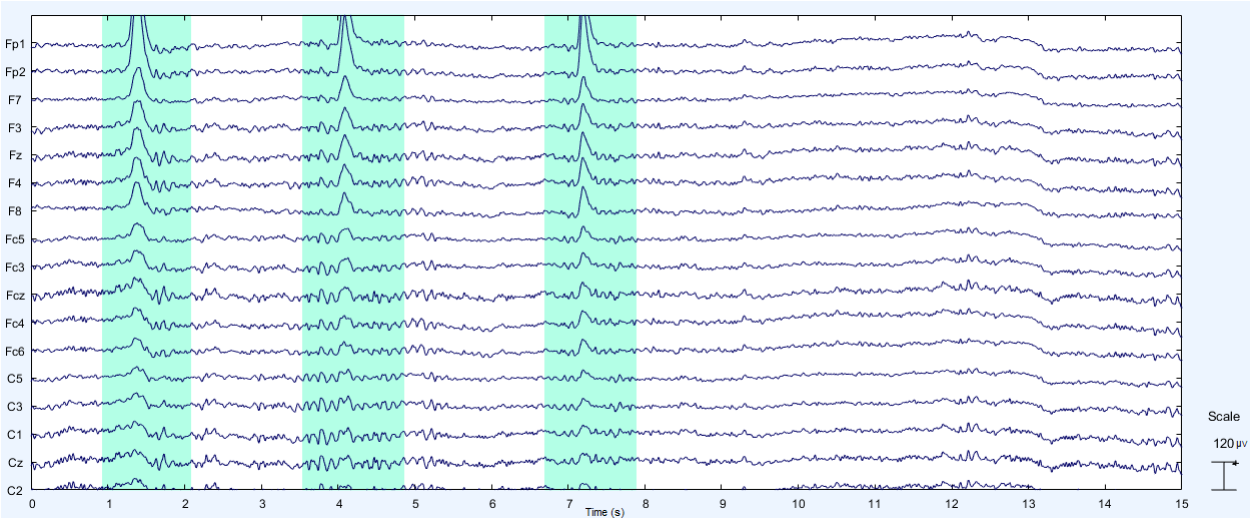

Figure 2.4: Typical blink eyes artifacts marked in cyan

Eye movements. Electrooculographic (EOG) activity is an electrical activity produced by eye movements, and it is considered as an artifact when EEG is recorded. EOG is generated by a frictive mechanism that is similar to the one described above for eye blinks, except that it involves the retina and cornea rather than cornea alone. The effect on frontopolar and frontotemporal electrodes can be symmetric or asymmetric, depending whether the movement is vertical or horizontal, respectively.
The effect of eye movement artifacts on frequency- or time-domain analysis is quite similar to that of blink artifacts, except that their frequency content is even lower, and amplitudes tend to be larger (Fig. 2.5). There exists current regression algorithms to remove EOG activity from EEG recording and other methods like ICA. A drawback in regression algorithms is that some extra electrodes need to be put on the face.

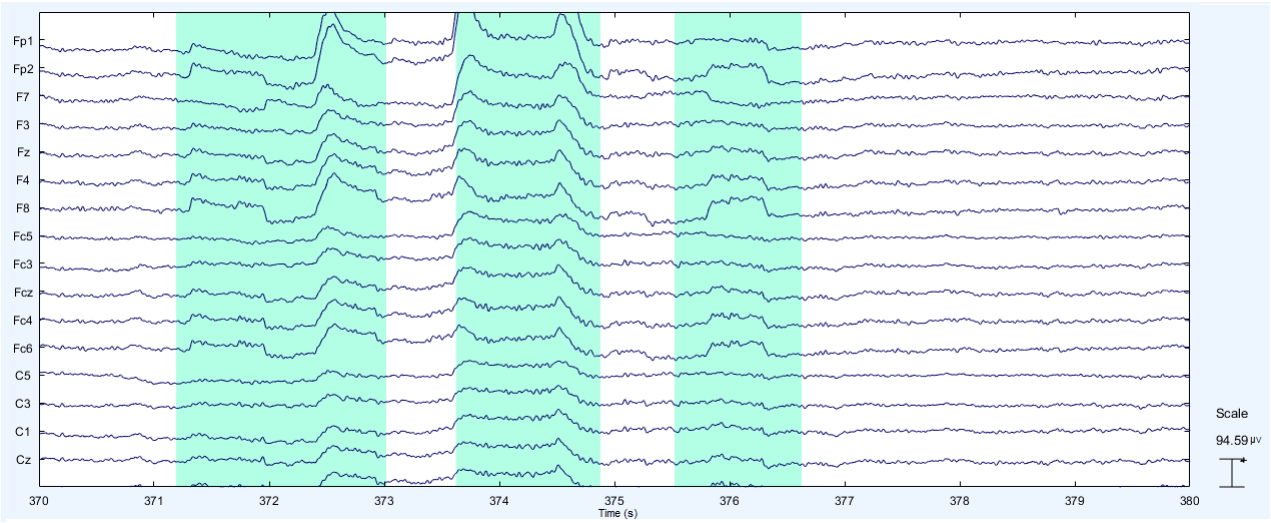

Figure 2.5: Eyes movement artifacts.

2.3.2 Temporal Filtering

Temporal filtering, also known as frequency or spectral filtering, is one of the first stages in signal preprocesing. This filtering is implemented with high-pass/low-pass/band-pass filters or notch filters. Its main purpose is reject artifacts existing in specifics frequencies or insulate certain brain activities. For example, the lower frequency signals are generally related to eye blink (see fig. 2.4) and other artifacts such as amplifier drift or changes in skin resistance due to sweat; hence, the lower frequency brain signals are generally high-pass filtered to remove the noise [39].
Nevertheless, temporal filtering in low band can also be used to retain brain signals; for example,limbs movements are decoded by Slow Cortical Potentials (SCP), thus a band-pass filter is needed in a low and narrow band of 0.1 -4 Hz.
Furthermore, band pass filters are applied to extract the components representing motor imagery from the brain signals in a specific frequency band such as the mu and beta bands. In Sensory Motor Rhythms BCIs, EEG signals are generally temporally filtered using a pass band filter between 8-30 Hz.
Linear finite impulse response (FIR) filters are sometimes used in EEG analysis. To ensure that phase delays introduced by the filter are nullified, an usual technique consists in applying the filter forward and then again backward. Infinite impulse response (IIR) filters like Butterworth, are also widely used for BCI preprocessing. Although IIR filters usually introduce different phase delays at different frequencies, this is compensated by the same technique of applying filtering in reverse. Many times, IIR filtering is preferred as they are very efficient, stronger and shorter than FIR filters.

2.3.3 Spatial Filtering

Spatial filters derive signal features by combining data from two or more locations so as to focus on activity with a particular spatial distribution. The main motivations of their implementation in BCI, are reducing spatial blurring effects, improving signal to noise ratio (SNR) and source localization in EEG.
Most of spatial filtering methods in BCIs consist in a linear map. Since EEG record consists

in a multi-channel recording obtained from different spatial locations, a linear combination of original channels leads to obtain new virtual channels or independent components, *i.e.* a mapping from sensor space to components space. The set of coefficients of the channels defines a spatial filter. Spatial filtering applied to EEG record is mathematically modelled as a linear map by:

$$y(t) = W\ x(t) \tag{2.2}$$

Where:
$x(t) = [x_1(t),\ x_2(t), ..., x_n(t)]$ are the recorded EEG n-signals. It can be in the matrix form as $X \in \mathbb{R}^{ch\ x\ sample}$, whose dimension is number of channels by time samples and $rank(X) = n$.
$W \in \mathbb{R}^{ch\ x\ ch}$ is the transformation matrix, that is the spatial filter applied on the multi-channel signal x. This matrix W is obtained by the various spatial filtering methods, and its rows contain the filter coefficients.
The values of the columns of the inverse of the transformation matrix,W^{-1} , determine the contributions of each individual component from the channels in the signal space. Thus these values and the topographic information of the channels can be used to generate the so called scalp or topographic maps [39].

Laplacian and CAR filter

Some of the simplest yet practical spatial filters are Laplacian spatial filter and Common Average Reference filter. As they are very similar in implementation, both are describe next.

Laplacian Reference The Laplacian derivation is the second spatial derivative of the two-dimensional Gaussian distribution on the scalp surface, and thereby emphasizes activity in radial sources immediately below the recording location. It can be computed by combining the voltage at the location $s_n(t)$, in each instant of time t, with the average voltage of surrounding electrodes $s_i(t)$; as shown in next equation:

$$s'_n(t) = s_n(t) - \frac{1}{m}\sum_{i \in S_i} s_i(t) \tag{2.3}$$

There are two typical Laplacian references: small and large (see fig.2.6). The small Laplacian reference subtracts the averaged EEG signals of the nearest four electrodes from the signal being preprocessed (for equation above $m = 4$); while in large Laplacian reference, the average of the next nearest four electrodes are are subtracted ($m = 8$ in equation above).
As the distance to the surrounding electrodes decreases, the Laplacian becomes more sensitive to voltage sources with higher spatial frequencies (i.e. more localized sources) and less sensitive to those with lower spatial frequencies (i.e. more broadly distributed sources) [40]. The Laplacian method is effective in reducing noise that should be more focused at a specific region.

Common Average Reference (CAR) The common average reference (CAR) method adjusts the signal at each electrode by subtracting the average of all electrodes (see Fig. 2.6(c)).
Implementation of this filter is modelled by Eq. 2.4. The potential $s_n(t)$ of each electrode n at each time point t is re-referenced to an estimated reference that is calculated by averaging the signals from all N recorded channels [39].

$$s'_n(t) = s_n(t) - \frac{1}{N}\sum_{i=1}^{N} s_i(t) \tag{2.4}$$

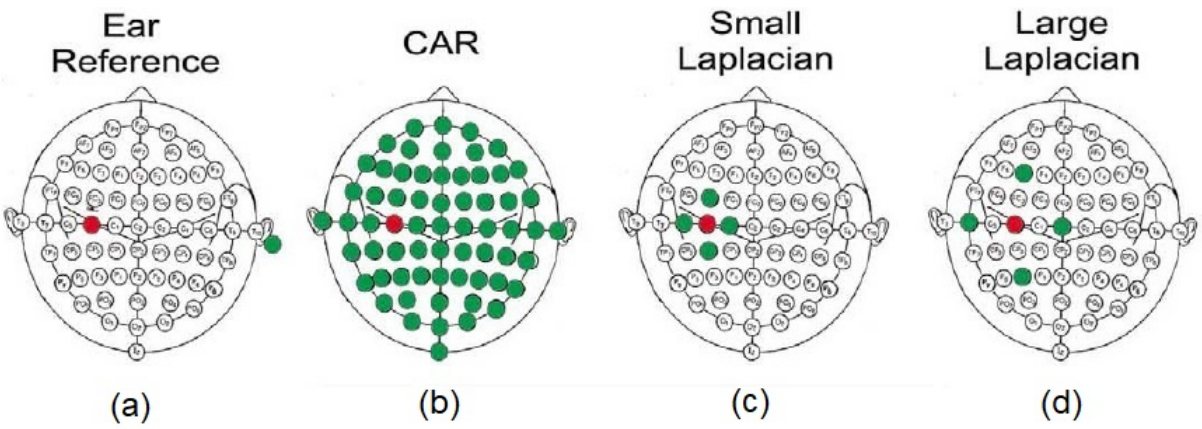

Figure 2.6: Differents spatial filters applied in C3 (marked as red electrode). Green electrodes are considered to compute C3.(Picture redrawn from [40])

Independent Component Analysis (ICA)

Independent Component Analysis (ICA) is a method that separate the brain signals into components, performing a brain source separation. To better explain this method, we refer to the so called "cocktail party problem" that consist in a room where people speak simultaneously and a person has to turn off the other voices and pay attention to only one conversation. Assuming that there are n persons speaking $s_1, ..., s_n$, recorded from n microphones $x_1, ..., x_n$ at different locations. Each microphone records a linear combination of all sources:

$$x_1(t) = a_{11}\ s_1 + a_{12}\ s_2 + ... + a_{1n}\ s_n \tag{2.5a}$$

$$x_2(t) = a_{21}\ s_1 + a_{22}\ s_2 + ... + a_{2n}\ s_n \tag{2.5b}$$

$$\vdots$$

$$x_n(t) = a_{n1}\ s_1 + a_{n2}\ s_2 + ... + a_{nn}\ s_n \tag{2.5c}$$

The analogy with brain signals is that n electrodes measure signals coming from many neurons. It is assumed that there are n mutually independent but unknown sources in

the brain signals denoted as $s(t) = [s_1(t), ..., s_n(t)]^T$ producing the n observable mixtures $x(t) = [x_1(t), ..., x_n(t)]^T$ in EEG recording. We have then:

$$x(t) = A\ s(t) \tag{2.6}$$

A is called the mixing matrix, which is often assumed to be full rank with n linearly independent columns. As can be seen from Eq. 2.2, the ICA algorithm computes a W transformation matrix (called demixing matrix), to be applied over brain signals $x(t)$ so that independent components $y_1, ..., y_n$ obtained, denoted as $y(t) = [y_1(t), ..., y_n(t)]^T$ are statistically independent.

ICA method is very useful to reject undesired independent components corresponding to artifacts (such as eye blink components or ocular movement components) and retain independent components related to EEG activity. The remained components are projected back into the signal space by:

$$\hat{x}(t) = W^{-1}y(t) \tag{2.7}$$

2.4 Feature Extraction

Once signal to noise ratio has been improved, in order to decode user's intent, representative features are extracted from neural correlates associated to user's intent. Later, these features can be exploited by a classification stage. We review in this section feature extraction techniques and considerations related to decoding of motor activity for BCI.
A great variety of features have been attempted to design BCI such as amplitude values of temporal signals, Band Powers, Power Spectral Density (PSD) values, AutoRegressive (AR) and Adaptive AutoRegressive (AAR) parameters, Time-frequency features and inverse model-based features.

2.4.1 Feature properties

Concerning the design of a BCI system, some critical properties of these features must be considered [75]:

Time information: BCI features must contain time information when brain activity patterns are related to specific time variations of EEG. This is the case of time-locked signals like MRCP that occur in a specific time related to movement onset.

Channel information: BCI features should also contain channel information since user's intents are coded in distinct brain areas. In the case of decoding motor activity, it is mainly focused in motor cortex, thus feture vector may be form mainly from channels on motor cortex.

High dimensionality: In BCI systems, feature vectors are often of high dimensionality. Indeed, several features are generally extracted from several channels and from several time segments before being concatenated into a single feature vector. There are at least two reasons why the number of features should not be too large. First, the computational complexity may become too large to fulfill the real-time requirements of a BCI. Second, an increase of the dimension of the feature space may cause a decrease of the performance of the BCI system. This is because the pattern recognition methods used in BCI systems are set up (trained) using training data, and the BCI system will be affected much by those redundant or even irrelevant dimensions of the feature space. In these cases, a dimensionality reduction may be performed using PCA algorithm.

Distribution: Since many classifiers assume normally distributed features, the feature distribution must be transform to a more Gaussianlike shape. This is sometimes done by computing the logarithm of the features.

Noise and outliers: BCI features are noisy or contain outliers because EEG signals have a poor signal-to-noise ratio.

Non-stationarity: BCI features are non-stationary since EEG signals may rapidly vary over time and more especially over sessions.

2.4.2 Feature extraction concerning to motor decoding

The main aspect to be considered in feature extraction and selection for motor decoding, is that features must represent and capture the neural correlates of movements.
For example, when SMR are considered to decode motor activity, features must capture the ERD/ERS patterns related to motor activity. The most widely used features closely related to the concept of ERD/ERS are those formed by calculating the power in specific frequency bands, the so-called band power features.

In the case of MRCP as neural correlates of movement; it is know that movements are encode as slope, point of maximum negativity and latency of the MRCP morphology. Therefore, some common temporal features considered in a specific time window comprise amplitudes of the down sampled signal, point of maximum negativity, mean amplitude of the data window, slope and intersection of a linear regression of the data in the specific window, slope and intersection of a linear regression of the data in a specific window.
Others kinds of features are sometimes considered as phase features, spectral features or entropy-based features [70].

2.5 Classification

To validate, in neuroimage studies, a neural signature correlated to an user's intent as well as to translate features into device control commands in BCI applications; features are assessed through a classification stage.

There are several classification algorithms, belonging to the fields of machine learning and statistical learning, that can be applied in BCIs. The current algorithms most used in BCI applications are Linear Discriminant Analysis (LDA), Support Vector Machines (SVM)[47], Random Forests (RF) [46], hidden Markov model (HMM)[48] and Bayesian Nets.
It must be said that there is no a superior classification method. A classification approach may provide a better performance for a particular problem whereas other classifier could be better in others applications. However, in many cases, non-linear classification methods are preferred. In this section, LDA and SVM classifiers are briefly introduced.

2.5.1 Linear Discriminant Analysis (LDA)

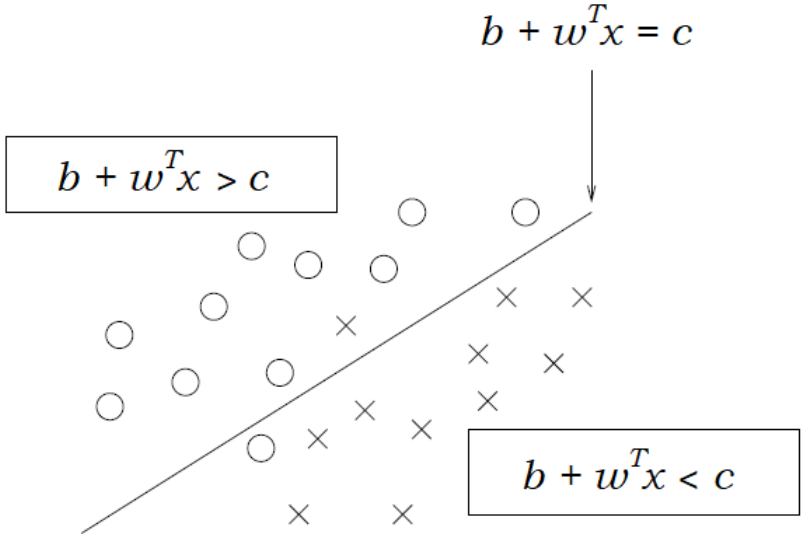

Figure 2.7: Two classes, the *"circles"* (class 1) and the *"crosses"* (class 2), are separated by an hyperplane obtained by LDA.

A linear classifier looks for a vector w and scalar b (line parameters), to separate data in two classes according to $w^T x + b \geq c$ for class 1 and $w^T x + b \leq c$ for class 2 (see Fig. 2.7). LDA method makes an optimal map from a high dimensional space to a lower dimensional space where data is easier to be separated. LDA also assumes a normal distribution of the data, with equal covariance matrix for both classes. The separating hyperplane is obtained by seeking the projection that maximize the distance between the two classes means and minimize the interclasse (within) variance. Thus, the optimization criterion is to maximize the ratio of between-class scatter to within-class scatter given by

$$J(w) = \frac{w^T S_B w}{w^T S_W w} \tag{2.8}$$

Considering S_1 and S_2 as covariance matrices of data belonging to class 1 and class 2

respectively; S_W matrix is computed by:

$$S_W = S_1 + S_2 \tag{2.9}$$

The between class scatter matrix for two classes, S_B, is constructed with the mean values m_1 , m_2 of each class data by:

$$S_B = (m_1 - m_2)(m_1 - m_2)^T \tag{2.10}$$

The scalar b is set to be:

$$b = \frac{1}{2} w^T (m_1 + m_2)$$

Finally, data is separated into each class, according to:

$$y = \begin{cases} -1 & \text{if } w^T x \geq b \\ +1 & \text{if } w^T x \leq b \end{cases}$$

2.5.2 Support Vector Machines (SVM)

The support vector machine (SVM) is binary classification method, *i.e.* it searches for an optimal hyperplane that separates the data into two classes. The best hyperplane to be found is the one with the largest margin between the two classes. Margin means the maximal width of the slab parallel to the hyperplane that has no interior data points. The support vectors are the data points that are closest to the separating hyperplane; these points are on the boundary of the slab (see Fig. 2.8).

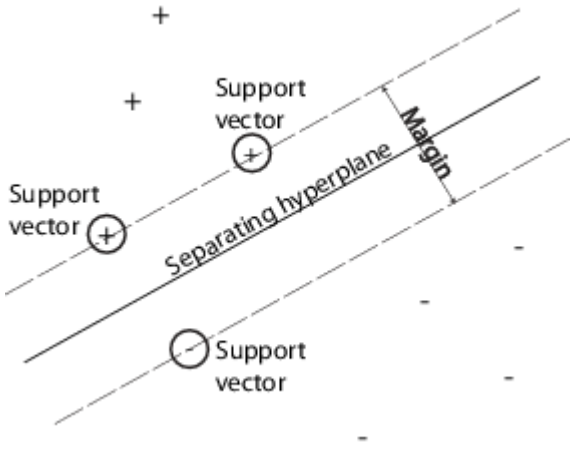

Figure 2.8: Hyperplane obtained by SVM. + correspond to data points of class 1, and - indicate data points of class 2. Support vectors are enclosed by circles ensuring a maximum margin and consequently an optimal separating hyperplane

For a linear SVM, the large margin (i.e. the optimal hyperplane w) is realized by minimizing the cost function on the training data:

$$J(w, \xi) = \frac{1}{2} \parallel w \parallel^2 + C \sum_i^n \xi_i \tag{2.11}$$

subject to the constraints:

$$y_i(w^T x_i + b) \geq 1 - \xi_i \tag{2.12a}$$

$$\xi_i \geq 0 \qquad \forall i = 1, ..n \tag{2.12b}$$

SVM algorithm solves this optimization problem through Lagrange multipliers.

For nonlinear SVM, the algorithm uses a "kernel trick", that consists in transform data into another space,generally of much higher dimensionality, using a kernel function $K(x, y)$. Formally said, is forming a Gram matrix using the predictor matrix columns. The dual formalization replaces the inner product of the predictors with corresponding elements of the resulting Gram matrix. Subsequently, nonlinear SVM operates in the transformed predictor space to find a separating hyperplane

2.5.3 Classifier assessment

The general performance of the BCI systems sometimes lies in the classifier performance. We mention now some techniques applied to ensure and validate classification performance.

K-fold cross validation

The former mentioned classification algorithms are supervised learning algortihms, it means that the whole data sets are divided into training set and test set. Training set is used to compute classifier parameters and then, the trained classifier is applied to test set. Cross validation is a model validation technique that aims to define a dataset to "test" the model in the training phase (i.e., the validation dataset), in order to limit problems like overfitting, give an insight on how the model will generalize to an independent dataset (i.e., an unknown dataset, for instance from a on-line BCI problem).
Cross validation may be computed either in an exhaustive or non-exhaustive way. The former case consists in learning and testing on all possible ways to divide the original sample into a training and test set. Since this validation is extremely large and computationally expensive, non-exhaustive methods are preferred. One of the most used non-exhaustive technique is K-fold cross validation. K-fold cross validation is performed by dividing the training set D into K equal parts denoted as $D_j, j = 1, ..., K$. In the j_th fold of the cross-validation process, D_j is used as a test test, while the remaining $K - 1$ parts are used as a training set. This procedure is illustrated in Fig.2.9 for a 5-fold cross validation.
Based on the predicted results at each "fold" and the true labels in D_j, a prediction accuracy rate r_j can be computed. Then, the K- rates are averaged to compute the final prediction accuracy rate r.

Classifier performance

In a motor BCI, the decoding of motor task is achieved by classification algorithms. Two classes classifiers are the most implemented, enabling detection of rest versus motion or motion versus motion.
A classification model is a mapping from instances to predicted classes. In binary discrete

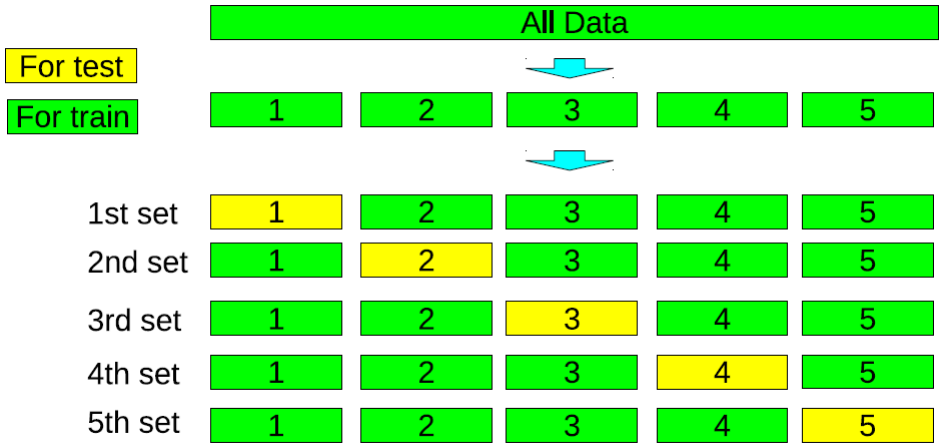

Figure 2.9: 5-fold cross validation procedure

classifiers, each instance $I \in \{P, N\}$ is mapped to one element of the set $\{P', N'\}$ of positive and negative class labels respectively.
Given a classifier and an instance, there are four possible outcomes. If the instance is positive and it is classified as positive, it is counted as a true positive (TP); if it is classified as negative, it is counted as a false negative (FN). If the instance is negative and it is classified as negative, it is counted as a true negative (TN); if it is classified as positive, it is counted as a false positive (FP). Given a classifier and a set of instances (the test set), a two-by-two confusion matrix (also called a contingency table) can be constructed representing the dispositions of the set of instances. It is shown in Fig.2.10.

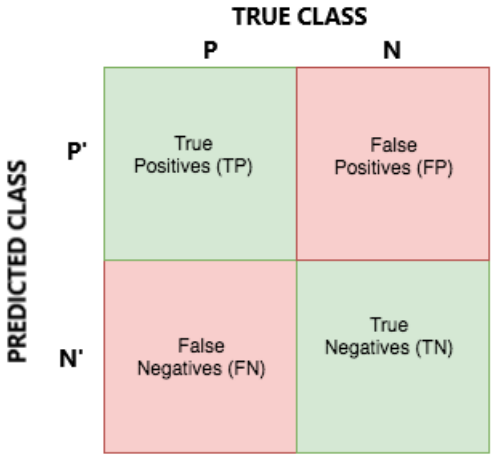

Figure 2.10: Confusion matrix of two class

The classifier performance can be measure by several common metrics that can be computed from confusion matrix.

Sensitivity (also called True positive rate (TPR) and recall) of a classifier is estimated as:

$$sensitivity\ (TPR) = \frac{positives\ correctly\ classified}{Total\ positives} = \frac{TP}{P} = \frac{TP}{TP + FN}$$

Specificity (also called true negative rate) of the classifier is:

$$Specificity\ (SPC) = \frac{negatives\ correctly\ classified}{Total\ negatives} = \frac{TN}{N} = \frac{TN}{TN + FP}$$

Precision (positive predictive value (PPV)):

$$PPV = \frac{TP}{TP + FP}$$

Accuracy (AAC):

$$AAC = \frac{TP + TN}{TP + FP + FN + TN} = \frac{TP + TN}{P + N}$$

Chapter 3

Methods

This chapter explains all stages developed in this thesis study, with the particular goal of decoding grasp from EEG, and within the general pursuit of designing a BCI for rehabilitation application. Experiment design is introduce at the beginning, followed by acquisition stage. The later sections comprise Neural correlates of grasping from EEG and Decoding grasp types.

3.1 Experimental Protocol Design

In order to find neural correlates of grasping and decode the performed grasp in EEG signals, we designed an experiment protocol taking into account the following considerations.

Importance of ADL. In the design of the experimental protocol, we were interested in replicate a scenario close to an everyday environment, as this might be the venue of possible BCI application. Furthermore, in rehabilitation context, the ecological validity of the therapy is increased if rehabilitation therapies are based on reproducible Activities of Daily Living (ADLs).
Most of our daily hand interaction with objects, involve three stages: hand approaching to the object, grasp it and performance an action with it. Thus, we designed a experimental protocol that consists in replicate an Activity of Daily Living (ADL)of reaching, grasping and open a door handle (see Fig.3.1).

(a) (b)

Figure 3.1: A daily living activity of opening a door. **(a)** Force grip performed to open a door.**(b)** Precision grip performed to lock a door.

Types of grasp There exists several studies concerning to grasp anatomy and taxonomy [58] [50] [51] [52]. Despite of the large number of grasp taxonomies, we select a quite general one,consisting of two kind of grasp, to be known, force grasp and precision grasp. Furthermore, others neuroimage studies about grasping also consider these two grasps [53] [60] [63] [54]; thus we may contrast our results with them. To that aim, two kinds of door handles were placed in a door. They were selected to perform these two general kinds of grasping, force and precision grasping.

Isolating grasp action Motor activity is encoded in low EEG signals. As we are interested in grasp action, we investigate neural correlates in delta band (0-4 Hz); however, others muscular artifacts correlated with any grasp kind could lead to mistake results. In a functional grasping action several movements are integrated, such as elbow extension, shoulder abduction/adduction, shoulder flexion/extension, etc. Although we look for high-level commands that imply all these movements, we also want to isolate the grasp action; so we design a task where movements performed are the same in both task except for grasp movement.

3.1.1 Experimental setup and Instrumentation

The foregoing considerations were taken into account for experiment design. We next describe the experimental setup and the instrumentation implemented.
The subject begins in a rest position, seated comfortably in a chair about 50 cm from a table. A wooden board, simulating a door, was placed in the edge of the table. Two kinds of door handles were set in the wooden board, a door lever handle and a door lock handle (see Fig.3.2). A force grasp is performed to hold the former and a precision grasp to hold the later.

(a) (b)

Figure 3.2: Wooden board simulating a door, used in the experiment. **(a)** Door lever handle and a door lock handle. **(b)** Photodiode and push bottom instrumentation to detect each grasp time.

The distance between subject and object in table was determined for each subject in such a way that, movement of reaching the object with dominant hand was the most alike with the action of opening a door, at the same time that body movements other than hand reaching out were restricted.
Placement of each door handle with respect of hand reaching position and opening mechanism was arranged in order to isolate hold (grasp) movement from others. It means that

in each grasp choice, all movements performed in reaching stage were exactly the same except for grasp movement. Moreover, the twist opening action with either door handle was selected to be a wrist pronation movement of 45 degrees in both cases. Thus, only grasp action was different for each selection.

In order to know the exact time at which each action is performed, the following electronic instrumentation was equipped:

- **Reaching.** A photodiode was put in armrest to detect the time when arm was moving out from armrest,that is to detect the start time of reaching movement. This photodiode also let know the time when all action has ended, it is the start of rest period.
- **Grasp.** Both door handles were instrumented to have a detection trigger of the time of grasp. A photodiode and a push bottom were implemented in force handle and precision handle respectively.
- **Twist movement.** The door opening mechanism was adjusted with a limit switch in each one of the door handles. This allow us detect the twist event. We also equipped both mechanisms with an inertial measurement unit (IMU)

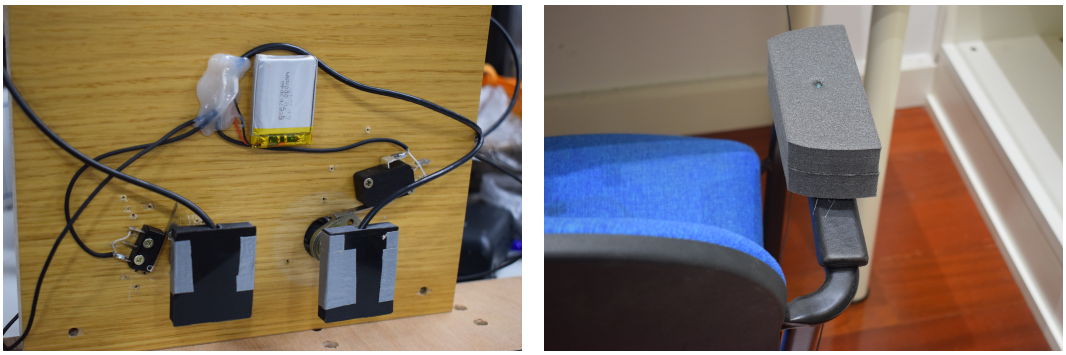

(a) (b)

Figure 3.3: **(a)** Switches and IMUs to detect movement for both grips. **(b)** Photodiode on arm rest. It detects reaching time and go back to rest moment.

3.1.2 Experimental protocol

The subject begins in a rest position then, at time desired by the user, he/she has to perform the complete action of reaching one of the two door handles, grasp it and twist it performing opening door. Once the action is done, subject has to return to rest position, staying in this position as much as is desired but with a minimum of 2 seconds.
The complete motor task has to be performed in a slow but natural way, emulating the opening of a door. This motor task is performed several times during 15 minutes, comprising a run. The experiment consist of two runs.
Door handle choice is left to the user with the only request to try a balanced selection of door handle along experiment. It means that this experiment protocol is both self-choice

and self-paced. During rest time, dominant hand stay on chair armrest.
Throughout motor task, the subject is constrained to avoid as much as possible eye blinking and other movements not related to experimental task; however, during rest time, blinking was allowed.
To prevent gaze correlated with tasks, it was requested to maintain gaze toward center of wooden board. Also, door handles position were interchange at each run.

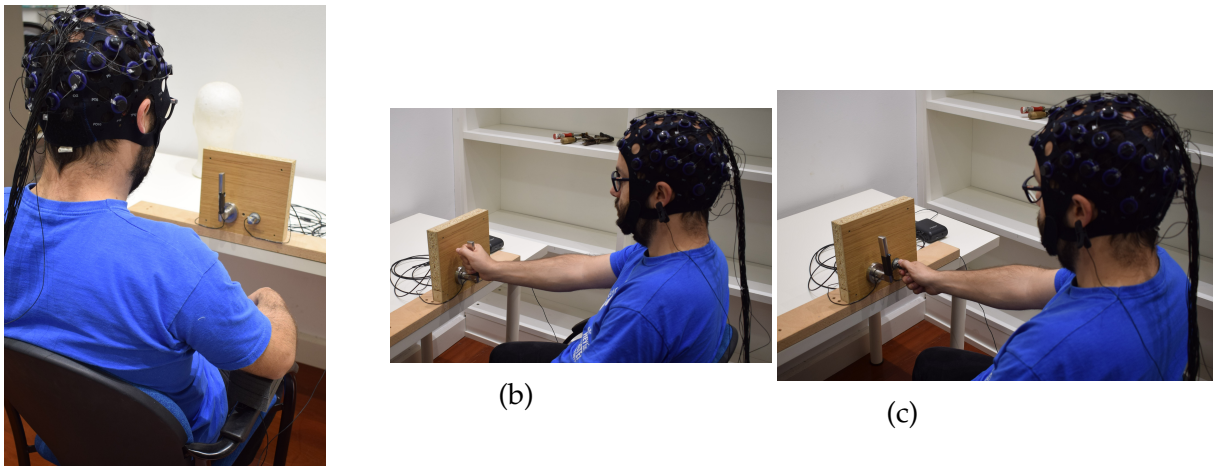

(a) (b) (c)

Figure 3.4: **(a)** Subject in rest position. **(b)** Force grasping performed. **(c)** Precision grasping performed.

Figure 3.5: Experimental setup.

3.2 Data Acquisition

Signal Acquisition

We record EEG brain activity at a sampling rate of 256 Hz, with a BitBrain Technologies® EEG 32-channels amplifier (see Fig. 3.7.b).
The 32 electrodes were placed covering frontal, central and parietal cortex regions; in the following positions, according to the to 10–20 System (see Fig. 3.6): Fp, Fp2, F7, F3, Fz, F4, F8, FC5, FC3, FCz, FC4, FC6, C5, C3, C1, Cz, C2, C4, C6, CP5, CP3, CPz, CP4, CP6, P7, P3, Pz, P4, P8, PO3, PO4, Oz
Reference electrode was placed in the left ear mastoid (A1) and Ground (Gnd) electrode in AFz position. We choose this electrode position arrangement in order to have a spatially distributed recording and a good spatial resolution over motor cortex.

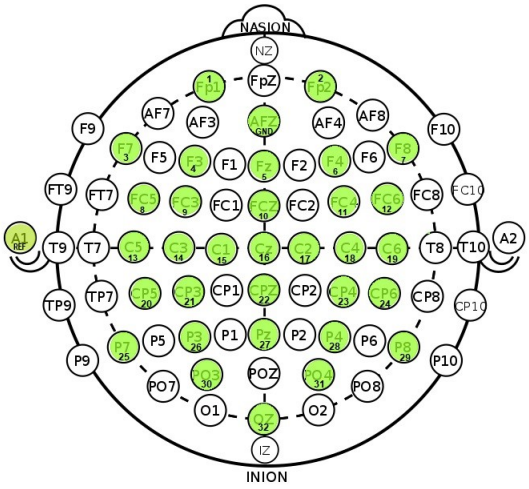

(a)

(b)

Figure 3.6: **(a)** Arrangement electrodes selection. Electrodes positions according to 10–20 System. **(b)** EEG cap with water electrodes in the selected arrangement.

Instrumentation signals were also recorded at a frequency of 256 Hz by Biosensig® , another BitBrain Technologies® device (see Fig.3.7(a)).
Both devices, Biosensig® and 32-channel EEG amplifier, send their records to a computer via bluetooth. In order to synchronize both recordings, a digital signal is sent from Biosensig® to the EEG amplifier. Since both records are sampled at same frequency, to synchronize both records it is just necessary to find the delay between them. This is achieved by computing a cross correlation between the digital output from Biosensig® and the digital input in EEG amplifier. The cross correlation of the two measurements is maximum at a lag equal to the delay between signals.

(a) (b)

Figure 3.7: **(a)** Biosensig®. Instrumentation device used to acquire all instrumentation signals from experimental setup. **(b)** 32 channels EEG amplifier by BitBrain®. Used to record EEG signals.

Subjects

For this study, ten healthy participants (age 30 ± 4 years, 8 male), all right-hand dominant, were recorded.
For every participant, we record two runs of 15 minutes each one. The average trials recorded per subject was 66 for precision grip and 67 for force grasps. The number of trials for each class and for each participant are shown in next table.
Note: Recording corresponding to subject 8 was omitted since experiment was not properly performed.

Subject	Force	Precision	Both grips
s1	83	77	160
s2	60	67	127
s3	31	34	65
s4	100	91	191
s5	54	67	121
s6	72	74	146
s7	54	47	101
s8	48	43	91
s9	49	58	107
s10	108	109	217

3.3 Neural correlates of grasping from EEG

This section comprises the EEG analysis performed in order to find neural correlates of grasping from EEG record. Offline processing of EEG and instrumentation data was performed using MATLAB R2015b (The MathWorks, Massachusetts, USA) with the EEGLAB toolbox [67].
We import the EEG record, composed of 32 channel signals; and we add events marks from experimental protocol. Latencies of these events are obtained from instrumentation signals. Therefore, we have the continuous EEG record with the following event marks:

1. **Reaching.** This is the latency when subject starts the task, reaching the object to be grasped from the arm rest.

2. **Force/ Prec.** Latency of grasp action. It can be either a force grip or a precision grip, depending on user choice.

3. **Mov. Force/ Mov. Prec.** Once the grasp is performed, the user the user twist the door handle, this time is also marked.

4. **Release.** Latency when door handle is released and subject returns to rest position.

5. **Rest.** Latency when all movement has finished and subject's arm is at rest position.

3.3.1 EEG preprocessing

We applied different preprocessing techniques pursuing the aim of obtain MRCP signals to be further analysed as neural correlates of grasping. Individual influence of each one of these techniques for the MRCP computation was analysed, as well as the integration of them in a preprocessing pipeline. We list next all of these techniques evaluated through this stage, even if not all of them were considered in our final pipeline proposition (see *Chapter 4. Results*). Later we explain our implementation of these techniques.

- Temporal filtering
- ICA
  - Manual component rejection
  - MARA rejection
- ASR cleaning
- Impedance check
- Spatial filtering
  - CAR
  - small Laplace

3.3.2 Temporal filtering

We perform first a band pass filter in the frequencies of $0.1 - 30Hz$ with the function $pop\_eegfiltnew$ from EEGLAB toolbox. It implements a Finite Impulse Response (FIR) filter using Hamming window. The upper limit is set at 30 Hz to remove high frequency artifacts such as muscular artifacts. The lower limit is keep in the extremely low value of 0.1 Hz to retain Slow Cortical Potentials.
Once the

Independent Component Analysis for artifact rejection

It is well know that eye related artifacts are present in low frequencies. Since we look for MRCP, that are low frequency signals as well; we must ensure the rejection of those artifacts. Once signals have been filtering, we perform an Independent Component Analysis over EEG signals to retain EEG activity components and reject undesirable components related to artifacts.

As it has been explained in section *2.3.3 Spatial Filtering*, ICA consits in a linear transformation that maps from EEG signals to independent components (ICs). We perform infomax ICA algorithm of Bell & Sejnowski (1995)[68] onto EEG record (see Fig.3.8) to

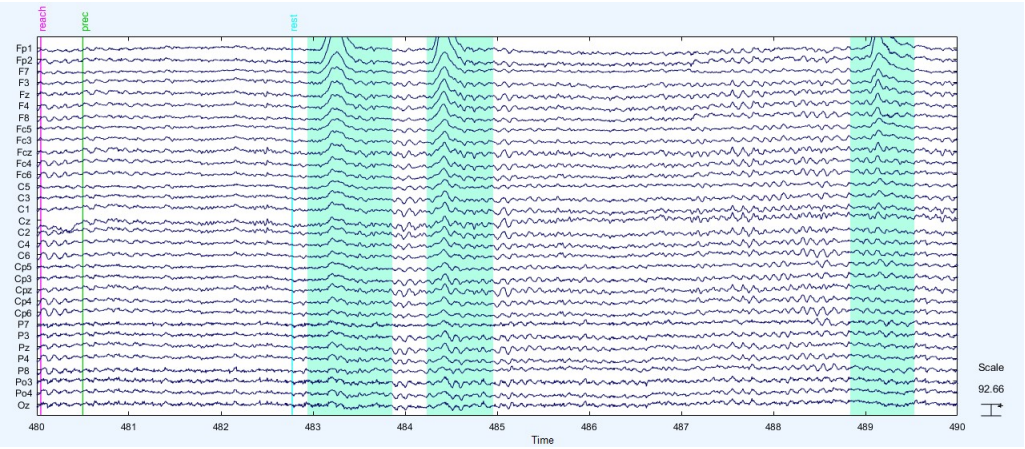

Figure 3.8: 32 channels EEG record (from 480 s to 490 s). Cyan areas mark the effect of eye blinking artifacts into record.

obtain an unmixing matrix W, the independent components (see Fig.3.9) are obtained by applying this unmixing matrix to the EEG signals as follows:.

$$U = WX(t) \tag{3.1a}$$

$$X(t) = [x_1(t), x_2(t), ..., x_32(t)]$$
$$U = [IC_1(t), IC_2(t), ..., IC_32(t)]$$

Since the EEG recording is composed by a linear span of all ICs, each one of these ICs may be seen as source generators of EEG. We can then extract the ICs related to blinks artifacts. We explain this procedure through the data set of subject 1. As it can be seen in Fig.3.9, the sixth IC seems to be the component that capture the blink artifact.

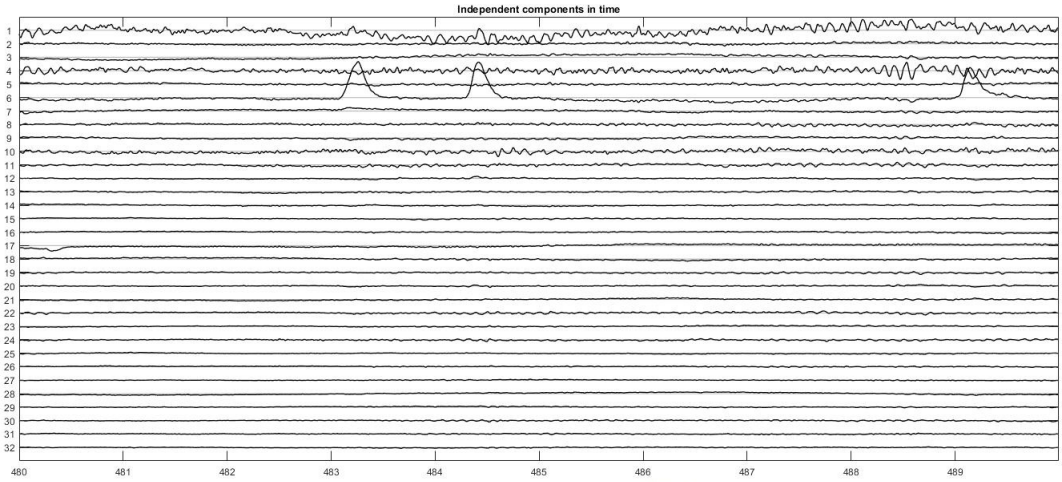

Figure 3.9: Time course (from 480s to 490 s) of Independent components obtained by ICA algorith. The sixth IC correspond to blink artifact

We additionally can plot the scalp projection of ICs (see Fig.3.10). These topographical representations are obtained by the columns of W^{-1}. It is seen in Fig. 3.11 that this sixth IC is mainly focused in frontal areas and from its activity power spectrum, there is no power

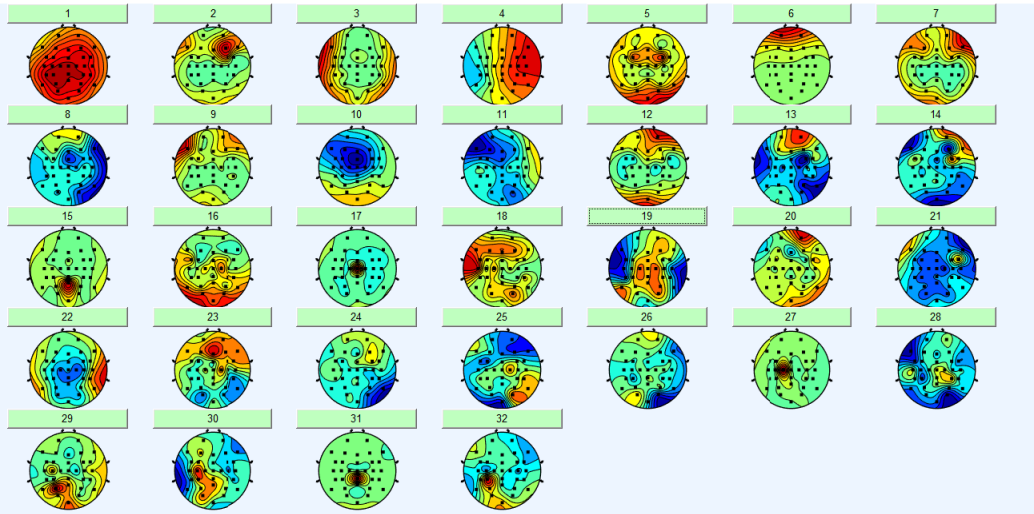

Figure 3.10: Scalp projection of ICs

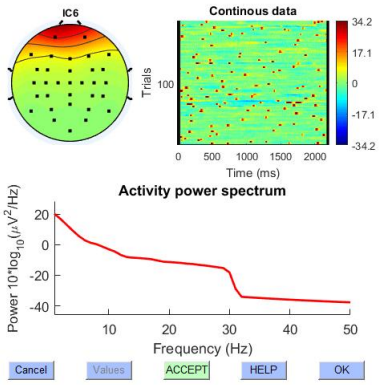

Figure 3.11: The sixth IC with its topographical representation and activity power spectrum.

peak in alpha frequency.
In order to clean EEG record, we extract this component related to an artifact and remap the remaining components from component space to channel space through the inverse of the unmixing matrix (see Eq.3.2).

$$\hat{x} = W^{-1}u \tag{3.2}$$

Since the original n channels are now reconstructed from $n-1$ sources, each component rejection derives in a loss of rank.
Component rejection can be performed by visual inspection of the scalp projections components time course and component power spectrum. However, a Multiple Artifact Rejection Algorithm (MARA) can be applied for automatic component rejection. We also test this algorithm in our experiments.
MARA extract six features from the spatial, the spectral and the temporal domain. Then,when supervised machine learning algorithm , using a large data base of features as training set, it performs a binary classification problem reject vs. accept.

Artifact Subspace Reconstruction (ASR) method

We test the Artifact Subspace Reconstruction (ASR) method [69] for cleaning EEG record. It is a strong cleaning algorithm, proposed originally for dry-electrodes and designed also for online aplications.
Volume conduction and scalp mixing are part of the nature of EEG recording, leading to high correlation between channels. It is normally seen as a drawback of EEG imaging; however, it is not at all, since signal channel reconstruction may be possible from neighboring channels. That is the main assumption exploit by ASR method. Although technical details that underline ASR algorithm are beyond the scope of this thesis, we explain in general steps how it works:

1. It finds a clean section of the data and uses it for calibration.
2. Principal Component Analysis (PCA) is applied on the continuous data with a 1 second slidding window.
3. Principal components (PCs) are classified into high variance and normal variance, with respect to calibration section. The threshold considered to classify PCs, can be set in a range between 3 - 8 standard deviations from calibration data.
4. Finally, ASR reconstructs high variance subspace (i.e. group of channels associated by a PC) with normal variance subspace. That is the reconstruction of a channel from adjacent channels.

In Fig.3.12 we illustrate implementation of ASR:

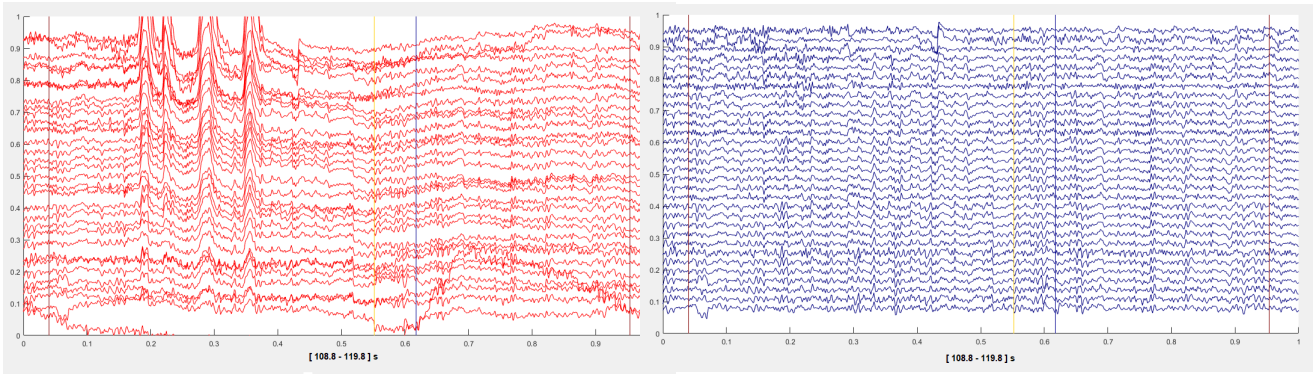

(a) (b)

Figure 3.12: Section from 108.8 -119.8 s of data record of subject 2. **(a)** Original signals. **(b)** Signals cleaned with ASR method.

SNR comparison of different spatial filters

For EEG, volume conduction is a problem that leads to recording of a blurred image of the actual underlying activity. Spatial filters are commonly applied to correct for some of this blurring and enhancing the SNR. For this thesis work, we also test the following spatial filters: ICA, Small Laplacian and CAR. Measuring their performance by Signal to Noise Ratio (SNR) value at the output of spatial filter.

First of all, we extracted signal and noise epochs from EEG continuous data record. Noise epochs were extracted from 2 seconds after Rest event mark, i.e. once all action has finished. Signals epochs were extracted from 2 seconds after reaching onset, considering most of the time of movement action. (see Fig.3.13)

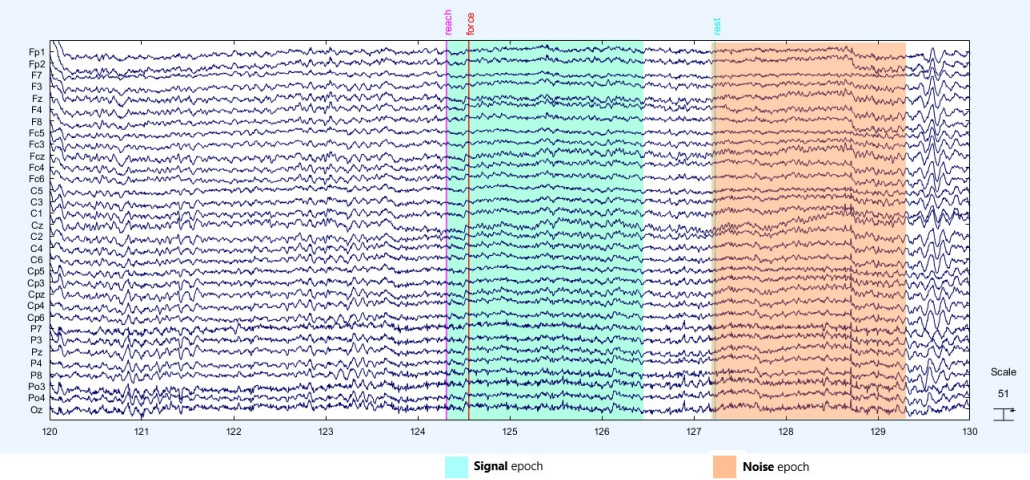

Figure 3.13: EEG recording with Noise and Signals epochs selection marked.

We compute SNR according to:

$$SNR = \frac{\sum_{l=1}^{L}\sum_{t=1}^{T}[x_S^l(t)]^2}{\sum_{l=1}^{L}\sum_{t=1}^{T}[x_N^l(t)]^2} \tag{3.3}$$

Where, L is the total number of epochs, T amount of samples in each epoch; $x_S^l(t)$ denotes the l- Signal epoch whereas $x_N^l(t)$ is the l- Noise epoch.
The better spatial filter performance is, the higher SNR value is expected.

Impedance check

We measure impedance across complete recording to know if an electrode lost contact during experiment. Moreover, since the complete recording for each subject is composed of two runs, we are interested in knowing if a channel has been lost from one running to another.
Impedance computation is performed offline. First, signals are filtered with a bandpass filter in a range of [70 - 90]Hz. Then, with a sliding windows, instant power is computed. Impedance is inferred from power value. We stablish a threshold (defined for BitBrain equipments) to determine if a channel lost contact during experiment. If a loss of contact is detected, we reject the channel and perform a channel interpolation.

3.3.3 MRCP

Once the EEG record have been cleaned of artifacts, we filter the EEG signals in a narrow band of $0.1 - 1\ Hz$. Since signals have been already filtered in a frequency band of $0.1 - 30\ Hz$, we just apply a lowpass filter with a cutoff frequency of $1hz$.

The MRCP is a time-lock signal, it means that it occurs in a certain time. Therefore we extract epochs in a window of $[-5\ 3]$s with respect of the reaching onset and then we performed a grand average over all the trials. As it can be seen in Fig.3.14, for both grip performed, typical negative deflection is observed prior to reach onset. EEG analysis implemented went beyond obtaining MRCP signals in a functional movement of grasping (reaching, object grasp and object manipulation). Through our experimental setup we time-locked signals to different mark events to observe its impact in MRCP morphologies. Furthermore, we analysed how MRCP signals, concerning to a functional movement, develops in time as a function of the time spent in each movement stage.

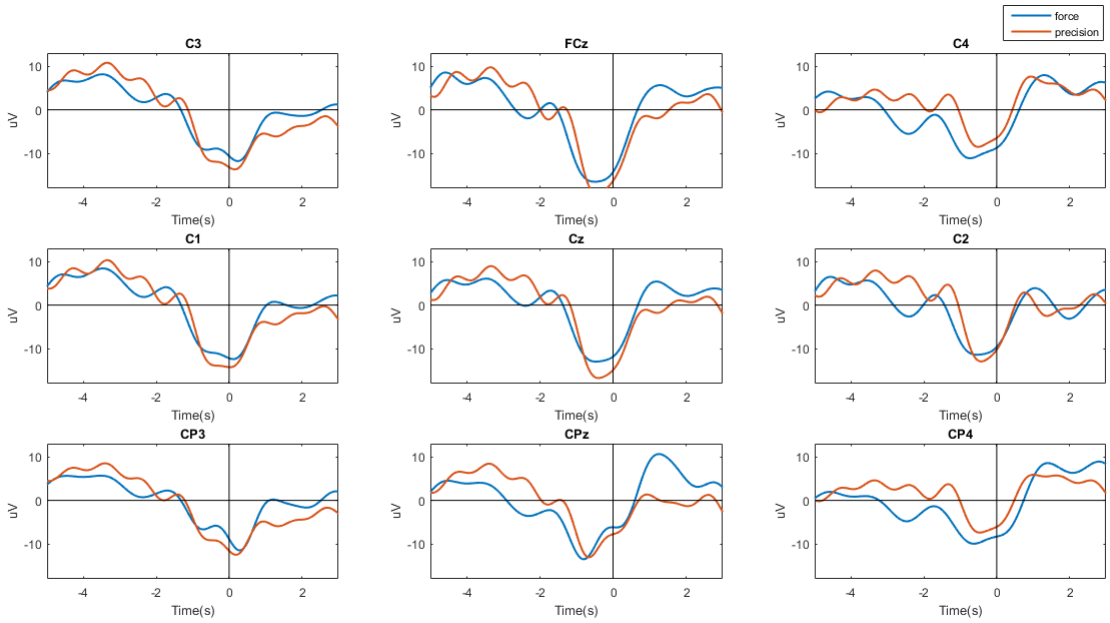

Figure 3.14: MRCP signals observed in centro-frontal, central and centro-parietal channels. Data corresponding to subject 2

3.4 Decoding of grasp

We analyse Movement related Cortical Potentials (MRCP) as EEG neural correlates of grasping. Two scenarios were assessed concerning to grasp decoding, both using single-trial classification:

1. **Grasp versus Rest.** Since one of the aims in this thesis is to find MRCP signals as neural signatures of grasping, we assessed this detection by a single trial classification between rest period versus grasping action. We implemented this classification stage using Linear Discriminant Analysis (LDA) as classifier. After signals had been preprocessing, we extracted the rest epochs from [0 2]s considering the rest onset. For grasp epochs, we extracted them from [-2 0]s with respect to the reaching onset. Two types of features were considered separately for this classification task, they were time features consisting of amplitudes and features obtained by Discriminant Spatial Pattern (DSP) filter.

2. **Force grip versus Precision grip.** Once the grasping action was detected we go beyond to analyse if grasp type is encoded in MRCP features. Therefore, we separated grasp epochs into two classes according the grip performed,i.e. force grip and precision grip. Three kinds of features were used separately for decoding grasp type. To be know: amplitud from time-locked signals, features obtained by DSP filter and phase features extracted from MRCP as well. Epochs for each kind of grip was formed from [-2 0]s with respect to the reaching onset. We used LDA classifier for this task. Adittionaly, for the feature with higher accuracy values we also performed a Support Vector Machine (SVM) with a radial basis function (RBF) as kernel.

We explain next the methodology followed for the three types of features considered for decoding.

3.4.1 MRCP Time Features

For time domain features, we down-sampled to 16 Hz the time-locked signals. Then we considered as features the amplitudes from channels over central and central parietal regions (C3, C1, Cz, C2, C4, CP5, CP3, Cpz, CP4, CP6) within window of [-2 0]s with respect to reaching onset.

3.4.2 MRCP Phase Features

Besides time-features extracted from MRCP, we also analyse phase features from MRCP; as it is suggested by some researches, these features present some advanteages in classification[72] [73].
First of all, time-locked amplitude signals before grand average for each channel $s(t)$, were decomposed by Hilbert transform into analytic representation.

$$z(t) = s(t) + iHT(s(t)) \tag{3.4}$$

Where $HT(s(t))$ is the Hilbert Transform, defined as:

$$HT(s(t)) = \frac{1}{\pi} P.V. \int_{\infty}^{\infty} \frac{s(t)}{t-\tau} d\tau \tag{3.5}$$

Where P.V. means Cauchy Principal Value. The former analytic representation of channel signals, can also be stated as a representation where instantaneous phase $\phi(t)$ and amplitude $A(t)$ components were explicit

$$z(t) = A(t)e^{i\phi(t)} \tag{3.6}$$

Furthermore, we compute the Phase Locking Value (PLV)[74]. PLV values were not considered as phase features in this thesis, however we introduce its computation and temporal evolution during grasp actions(see Fig.3.16).

$$PLV = \frac{1}{N} \mid \sum^{N} e^{i\phi} \mid \tag{3.7}$$

The phase features from MRCP that were taken into account to be exploited in classification, was Instantaneous Phase values of the signals down-sampled to 16 Hz, in a time window of [-2 0]s with respect to reaching onset and from 10 channels (C3, C1, Cz, C2, C4, CP5, CP3, Cpz, CP4, CP6). As it can be seen in Fig.3.15, among 5 representative subjects there is a consistent positive peak in prior information with respect to reaching. Furthermore, this priori positive peak is followed by a rebound leading to a negative peak with maximum negativity close to the reaching onset.

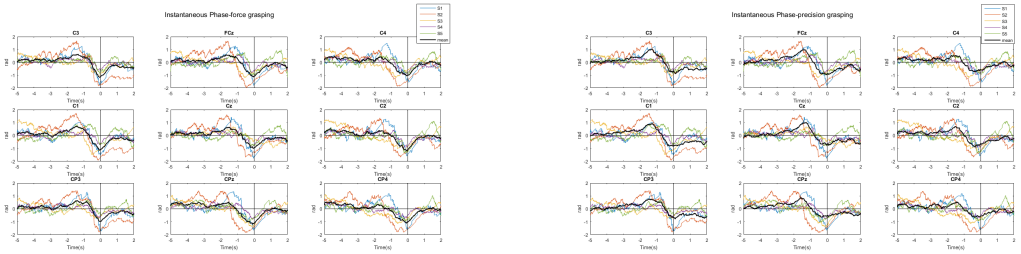

(a) (b)

Figure 3.15: Phase instantaneous value from MRCP. **(a)** Phase values for force grip among 5 subjects. **(b)** Phase values for precision grip among 5 subjects.

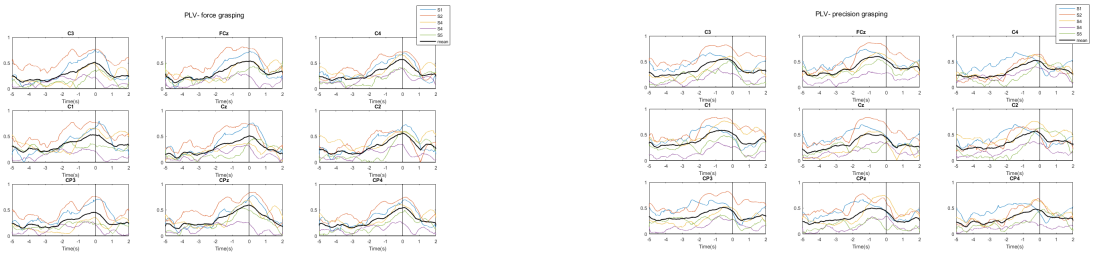

(a) (b)

Figure 3.16: Phase Locking values for both grips. **(a)** PLV in force grip. **(b)** PLV in precision grip.

3.4.3 Discriminative Spatial Patterns

When Sensory Motor Rhythms are considered to decode motor information, it is know that there are some optimal spatial filters, like Common Spatial Patterns (CSP), that have

been found to be very useful for ERS/ERD-based classification. However, CSP is not an appropriate approach for MRCP since they are slow nonoscillatory EEG potential shifts.
For the case when MRCP are used to decode motor information, there is another spatial filter suggested by Liao et. al, it is Discriminative Spatial Patterns (DSP) [71].
DSP algorithm is designed especially to detect the difference in the amplitudes of slow nonoscillatory EEG potentials. We applied this DSP filter in two cases, for decoding rest vs grasp and a second case of force grip vs precision grip. We explain next the methodology.
First we form trials of each one of the class, denoting $X_j(i)$ as the $i-$trial corresponding to class j. The number of classes will be denoted as K, so we have $K = 2$.
In our implementation, for the case of discrimination between two grips, we considered epochs of 2 seconds before the reach-event of each one of the class. For the case of detection of grasp, we form rest trials with 2 seconds after the rest-event and grasp trials with 2s before reach-event. We considered reach-events of both grips since in this case we are only interest in detect grasp with no matter which grip is performed.
Then we compute the conditional average of each class M_j:

$$M_j = \frac{1}{n_j} \sum_{i=1}^{n_j} X_j(i) \tag{3.8}$$

Where n_j is the total of trials of each $j-$ class.
Then we compute the within-class scatter matrix S_w and the between-class scatter matrix S_w. For the former:

$$S_j = \sum_{i=1}^{n_j} (X_j(i) - M_j)(X_j(i) - M_j)^T$$

$$S_w = \sum_{j=1}^{K} S_j \tag{3.9a}$$

For the between-class scatter matrix S_B:

$$M = \frac{1}{n} \sum_{i=1}^{n} X(i)$$

$$S_B = \sum_{ij=1}^{K} n_j (M_j - M)(M_j - M)^T \tag{3.10a}$$

We look for a discriminative projection matrix W which lead to maximize the projected class means at the same time as the classes variance is minimized. That is, project S_w and S_B as:

$$\hat{S_w} = W^T \, S_w \, W \tag{3.11a}$$

$$\hat{S_B} = W^T \, S_B \, W \tag{3.11b}$$

We posed this problem by the Fisher's linear discriminant criterion, i.e. looking for a W that maximize the ratio of the cost function:

$$J(W) = \frac{|\hat{S_B}|}{|\hat{S_w}|} = \frac{W^T \, S_B \, W}{W^T \, S_w \, W} \tag{3.12}$$

We can solve this problem by posing as a generalized eigenvalue problem:

$$S_B w_d = \lambda_d \, S_w \, w_d \tag{3.13}$$

Where λ_d is the eigenvalue and w_d is the column vector of W ($d = 1..N$). It may be solved by singular value decomposition (SVD). The solution of the generalized eigenvalue is a set of eigenvectors, i.e., spatial filters, and eigenvalues. The eigenvectors that correspond to the spatial filters are sorted in descending order of the eigenvalues. The DSP are obtained with columns of W^1 and they can be considered as time-invariant EEG source distribution vectors
Once the W have been found, we transform each single-trial EEG by:

$$Z_1(i) = W^T X(i) + w_0 \tag{3.14}$$

Where $w_0 = -W^T M$ is a bias term. The features are selected as the mean values of the DSP-based spatially filtered EEG. Considering the $r-$ first rows, the feature vector is composed as:

$$X^p(i) = \; mean\,(Z^p(i)) \qquad p = 1, ..., r \tag{3.15}$$

In our implementation we select $r = 2$, i.e. the two first rows.

3.4.4 Feature vector composition and dimensionality reduction

For both decoding scenarios, and for the three types of features; we extracted features from 10 channels on central and centro-parietal regions (C3, C1, Cz, C2, C4, CP5, CP3, Cpz, CP4, CP6). Features extracted from these channels were concatenated into a single feature vector.
Once feature vector was composed, to reduce dimensionality as well as to decorrelation method, we implemented a normalization of feature vector into range [0-1] and then we performed a Principal Component Analysis (PCA) in order to reduce the dimensionality keeping the 95% of the variance explained by PCA.

3.4.5 Classification

In this decoding stage of grasping movements, we contemplated two scenarios: The former, detection of grasp action with respect to rest. The second case was detection of grip performed between force and precision grip.
We exploit the previous features extracted for both cases through a classification stage. Two clasifiers were implemented, a Linear Discriminat Analyss (LDA) and a Support Vector Machine (SVM) with radial basis function as kernel. To avoid overfitting, we implemented a k-fold cross validation with 10 folds.
The classification scheme is as follows:

Empirical Chance level

In classification tasks, the results are expected to be above chance level; that is higher than a rate obtained by purely random classification. For a two-class task, this threshold is 50%. However, this theoretical chance level is based on the assumption of infinite number of

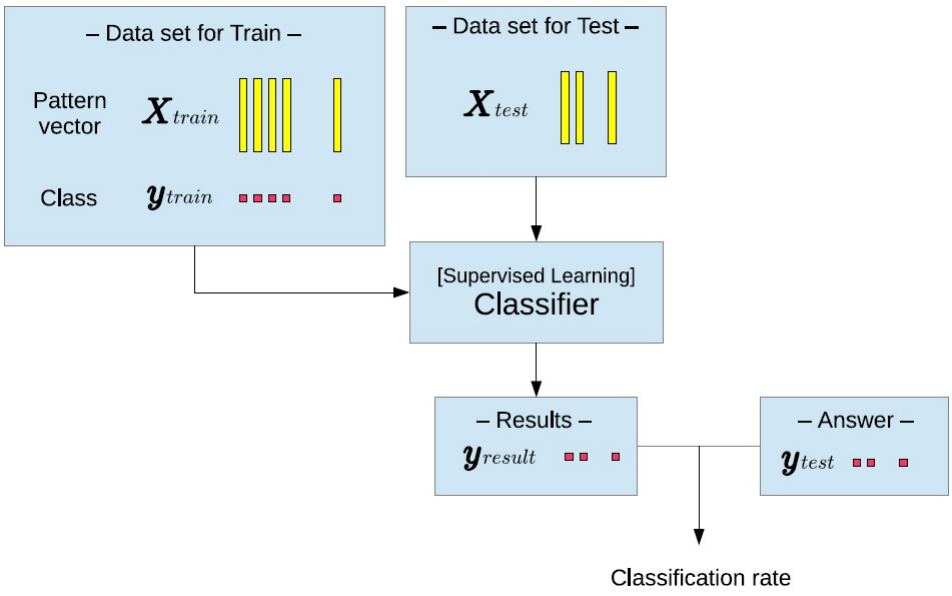

Figure 3.17: Classification scheme.

data samples. Therefore, for a small data set, an empirical chance level need to be computed based on trials available.
A way to overcome this issue is testing for the statistical significance of the decoding accuracy by derive a statistical significance threshold using a binomial cumulative distribution[76]. This approach assumes that the classification errors obey a binomial cumulative distribution, where for a total of n samples and c classes, the probability to predict the correct class at least z times by chance is given by:

$$P(z) = \Sigma \binom{n}{i} \left(\frac{1}{c}\right)^{i} \left(\frac{c-1}{c}\right)^{n-i} \tag{3.16}$$

Chapter 4

Results

4.1 Neural Correlates of grasping

4.1.1 Pipeline proposition

Our preprocessing pipeline for EEG analysis is presented in Fig.4.1. It includes some of the preprocessing techniques explained in section *3.3.1 EEG preprocessing*. Consideration taking into account for this pipeline are discussed in next chapter.

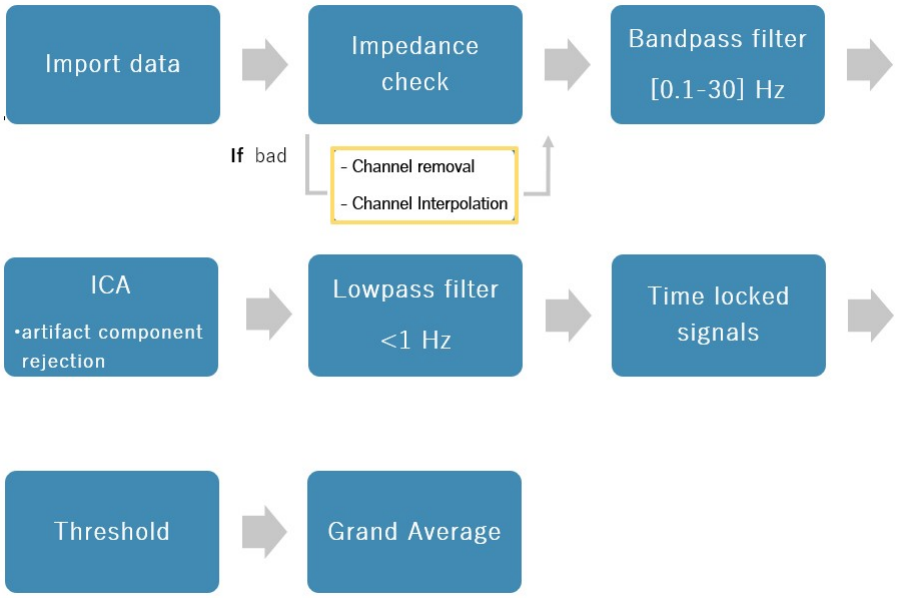

Figure 4.1: Preprocessing pipeline used for EEG analysis looking for MRCP in EEG record.

4.1.2 SNR comparison of different spatial filters

We present a comparison between different spatial filters. In order to consider which spatial filter using in our pipeline proposal we evaluate three different spatial filters, measuring their performance by the SNR at the output of the filter. For comparison purposes

we just shown 4 channels corresponding to channels were small Laplace was applied to. We evaluated these spatial filters for nine subjects.

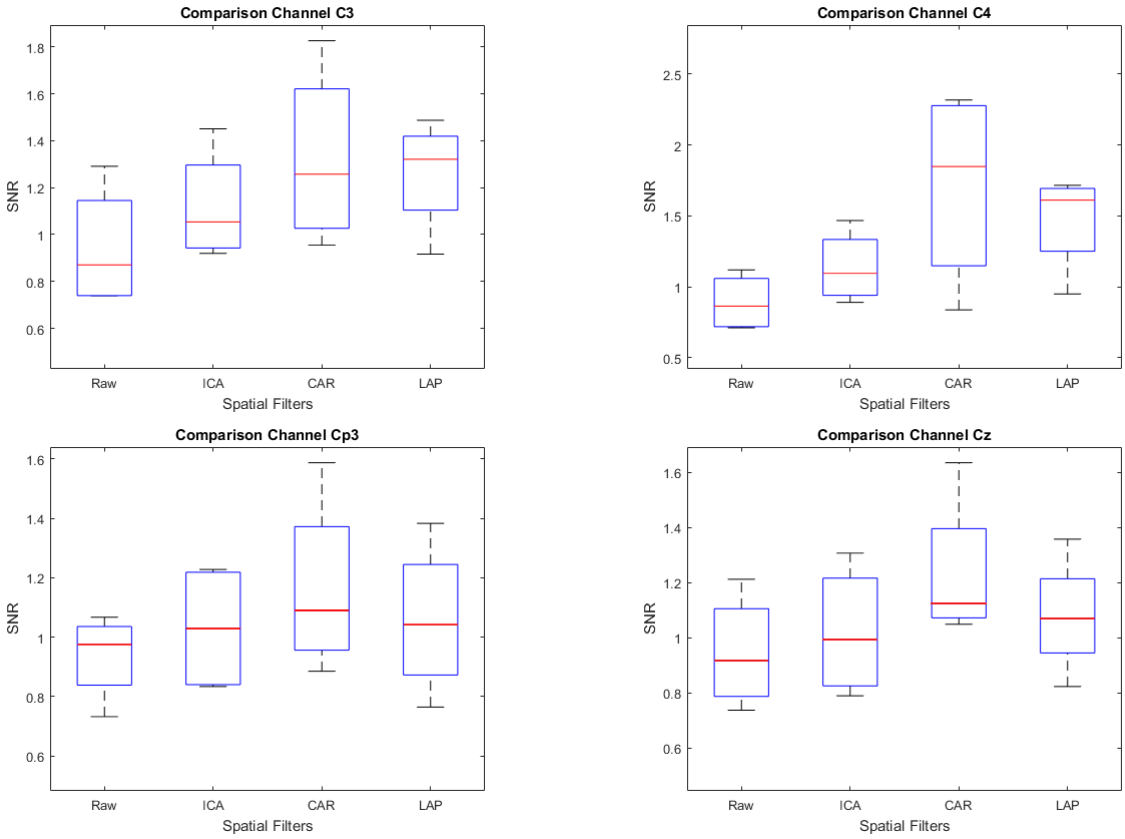

Figure 4.2: Evaluation of different spatial filters. Performance is measured by SNR.

4.1.3 MRCP in grasping

The experimental protocol was designed to find neural correlates of grasping. We introduce next the MRCP found for both cases, force grip and precision grip in a grand average across all subjects (see Fig.4.3). The typical MRCP morphology is observed in in all subjects as well as in the average across subjects (Fig.4.4).

4.1.4 MRCP develop across time

For three subjects, to be know those who performed less trials (S1, S3, S9), there were two MRCP morphologies during the time spent in performing the trial. By our experimental setup we know that second MRCP is time-locked to rest mark. This phenomenon is illustrated in figure 4.5

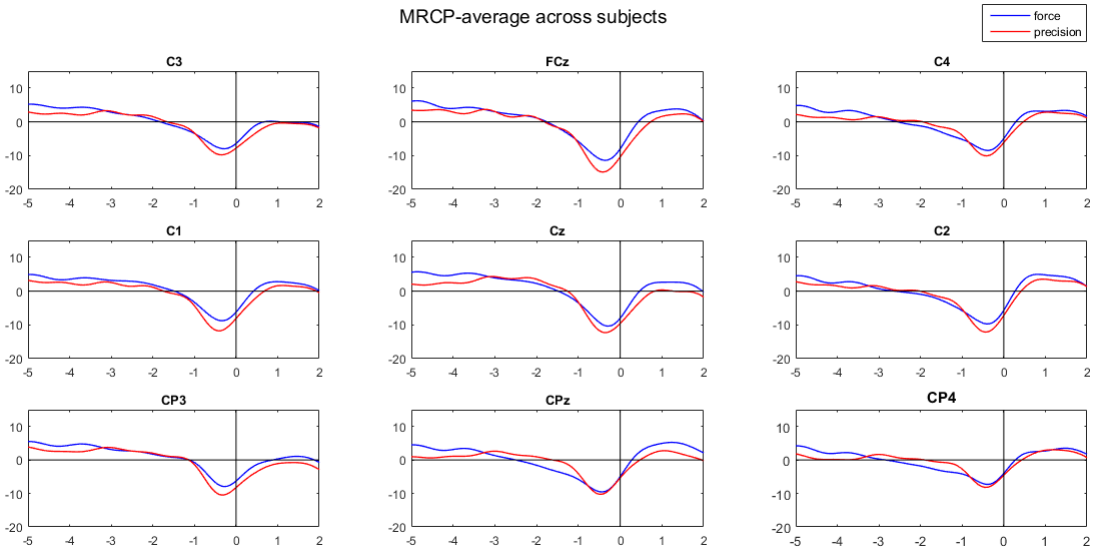

Figure 4.3: MRCP concerning to force grip and precision grip. This figure present the grand average across all subjects.

4.2 Decoding of grasp

4.2.1 Decoding rest versus grasp

We decode grasp versus rest using a LDA classifier considering two types of features independently: MRCP time features adn DSP features.
We also compute the empirical chance level considering the 95% confidence interval of the inverse of the binomial distribution for 137 trials. (That number of trials considered was set by the average across subjects of both grips performed). The empirical chance level computed was 56.93%.

MRCP time features

For MRCP time features considered as the amplitudes, we compute a total of 330 features, then we reduced dimensionality by retaining 95% of the variance explained by their principal components (PCA). The total of features after dimensionality reduction was 10 ± 3 features.
The average decoding performance accuracy obtained with this feature was 67.03% (average for all subjects). The accuracy together with the sensitivity and specificity rate; obtained for each subject is shown in Fig.4.6

DSP features

We additionally test DSP filter as it is suggested for MRCP features. We considered the two first rows of the signals filtered with DSP filter. Since we have only two features, no dimensionality reduction was compute although feature vector was normalize in the range [0-1].

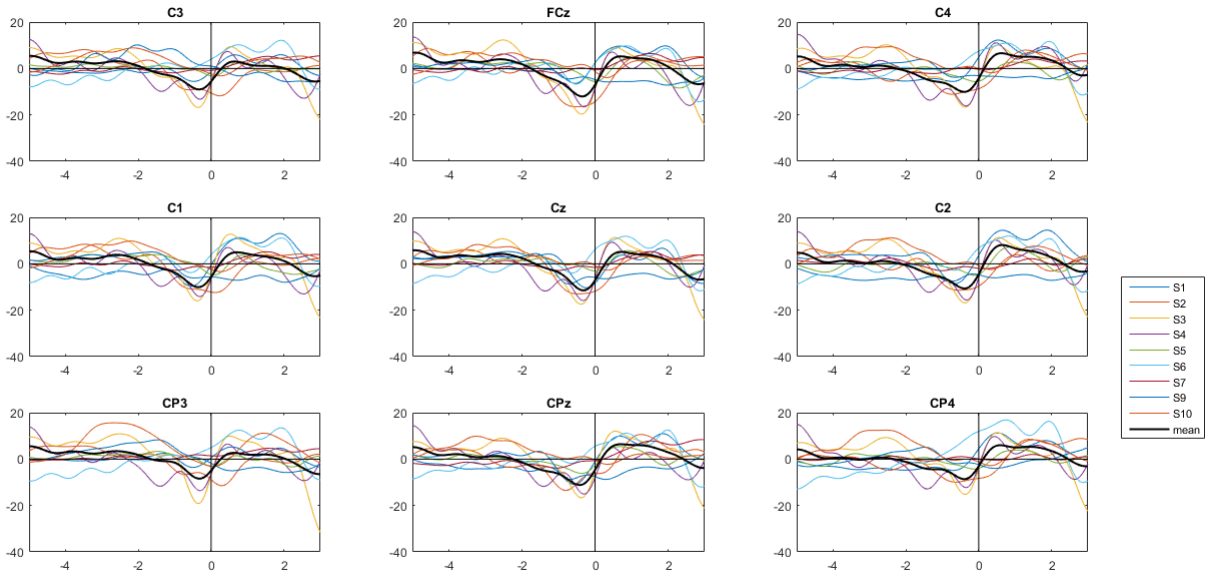

(a)

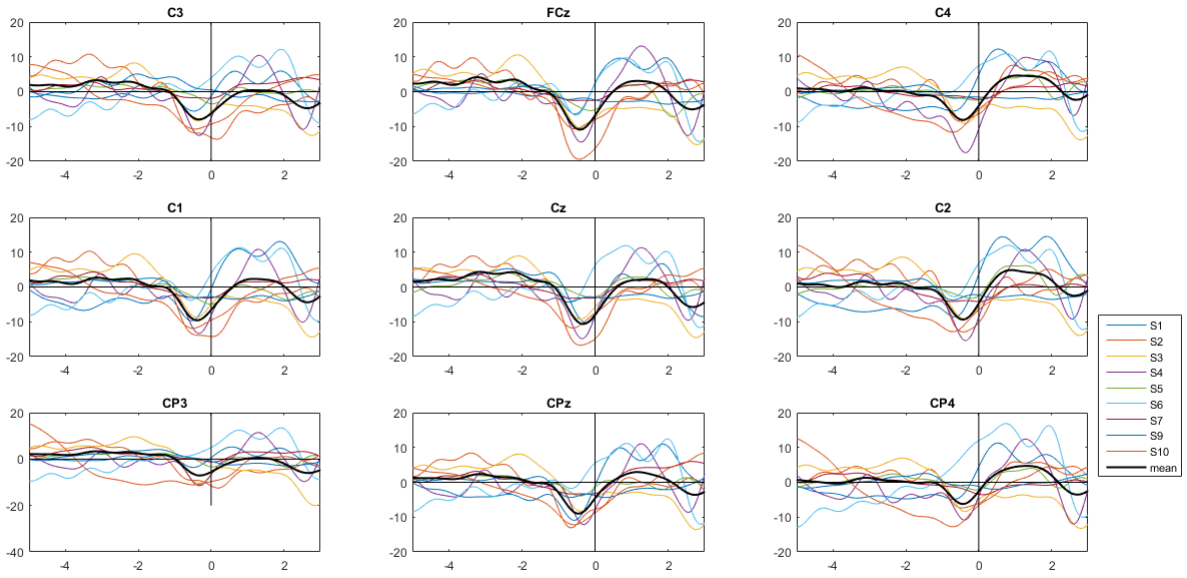

(b)

Figure 4.4: Time evolution of time-locked signals. (a)MRCP signals corresponding force grip and grand average across subjects. (b)MRCP signals corresponding precision grip and grand average across subjects.

The average decoding accuracy, using features obtained by filtering with DSP, was 76.74% (average for all subjects). The accuracy together with the sensitivity and specificity rate; obtained for each subject is shown in Fig.4.7

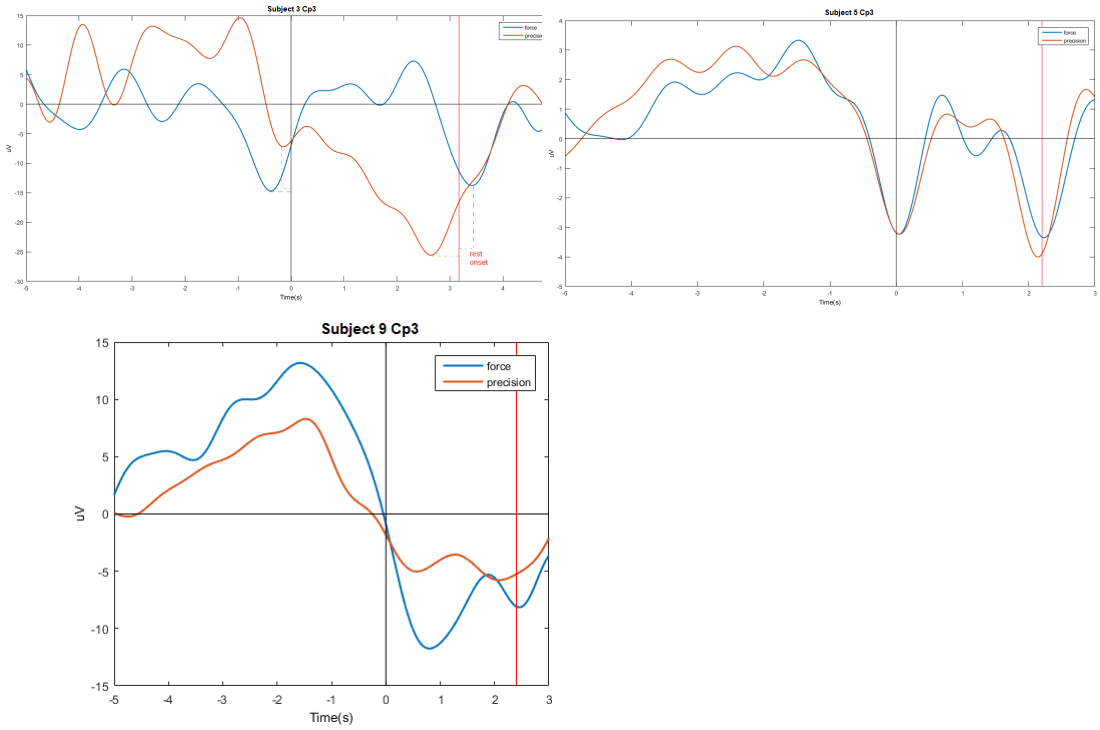

Figure 4.5: Two negative peaks were observed for three subject. MRCP signal corresponding to subject 3,5 (above) and 9 (below)

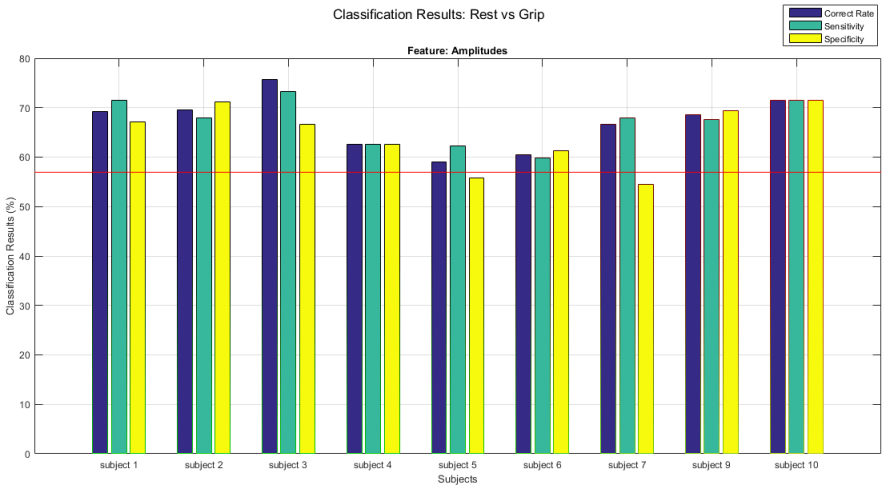

Figure 4.6: Classification results obtained for 9 subjects considered using amplitude as feature.

Features comparison

A comparison of the accuracy obtained using each feature is shown in Fig.4.8

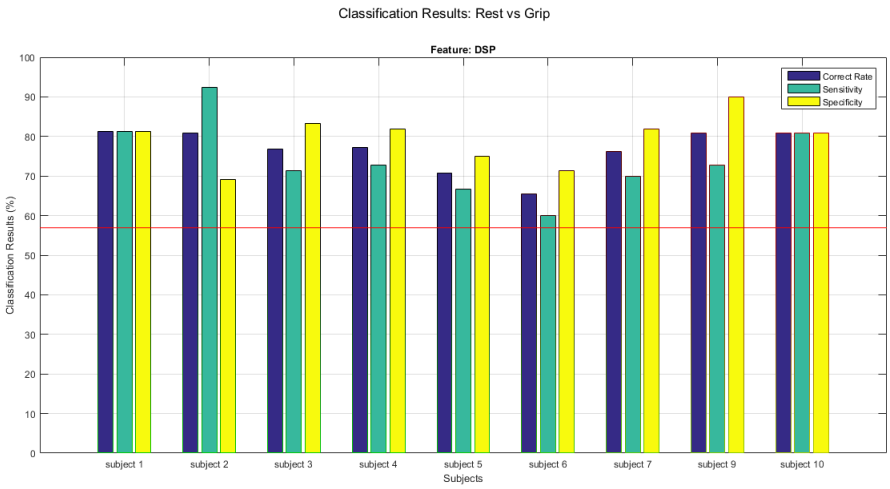

Figure 4.7: Classification results obtained for 9 subjects, using DSP features.

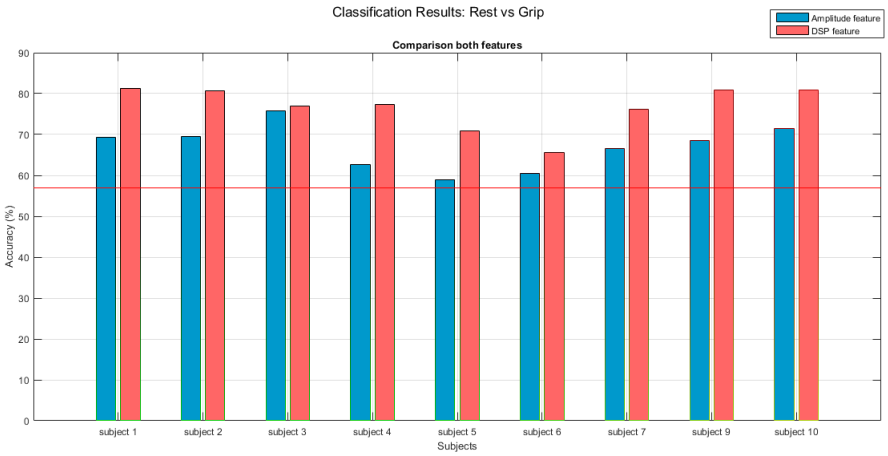

Figure 4.8: Comparison of accuracy obtained with each feature.

4.2.2 Decoding force grip vs precision grip

Beyond a classification between rest and grip, we decode type of grip using information prior to reaching onset. The same three types of features were exploited through a classification stage using a LDA classifier. Like in the previous scenario, we calculate empirical chance level taking into account 67 trials and considering the 95% confidence interval of the inverse of the binomial distribution. This computation give an empirical chance level of 60.29%

MRCP time features

A decoding between both grasp types was performing using temporal features, more exactly amplitudes of the epoch signals down-sampled to 16 Hz. Like in previous case, dimensionality was reduce by retaining 95% of the variance explained by PCA. The total of features after dimensionality reduction was 9 ± 3 features.
The average decoding performance accuracy obtained with this feature was 58.36% (average for all subjects). The accuracy together with the sensitivity and specificity rate; obtained for each subject is shown in Fig.4.9

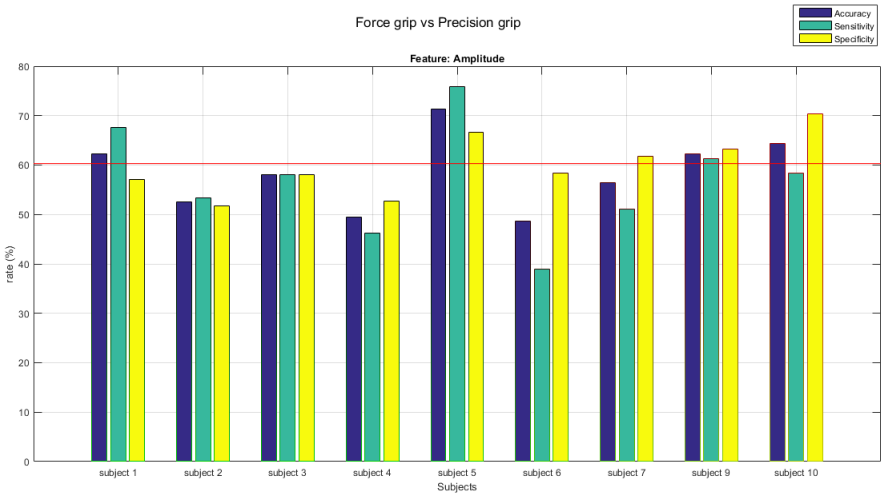

Figure 4.9: Classification results between force and precision grip using amplitude as feature.

Phase feature from MRCP

For decoding type of grasp performed, we also analysed phase features from MRCP. In Fig.4.10 we observe the grand average across subjects for the instantaneous phase obtained from MRCP signals. We also extract phase features from Instantaneous phase in

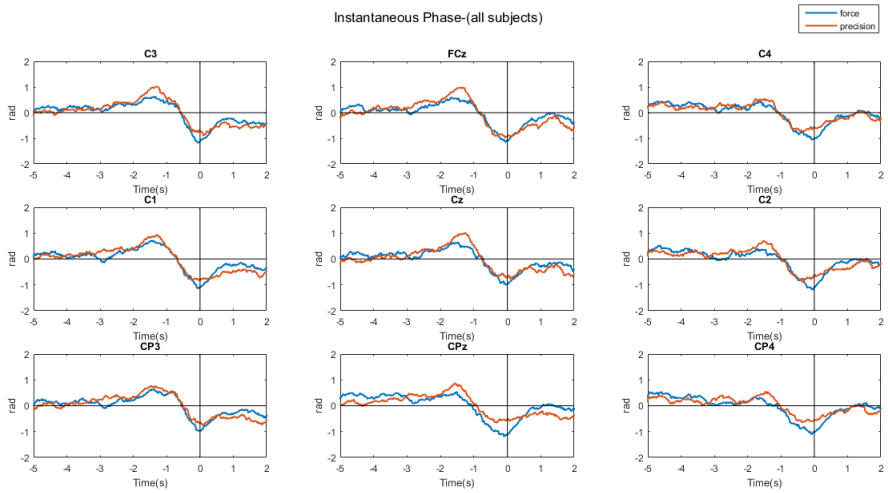

Figure 4.10: Grand average across subjects for Instantaneous phase value for precision and force grip.

a window of [-2 0]s with respect to reaching onset. We extract features from the same 10 channels considered for others features. The dimensionality was reduced as well by retaining 95% of the variance explained by PCA. The total of features after dimensionality reduction was 30 ± 10.
The average decoding performance accuracy obtained with this feature was 56.31% (average for all subjects). The accuracy together with the sensitivity and specificity rate; obtained for each subject is shown in Fig.4.11

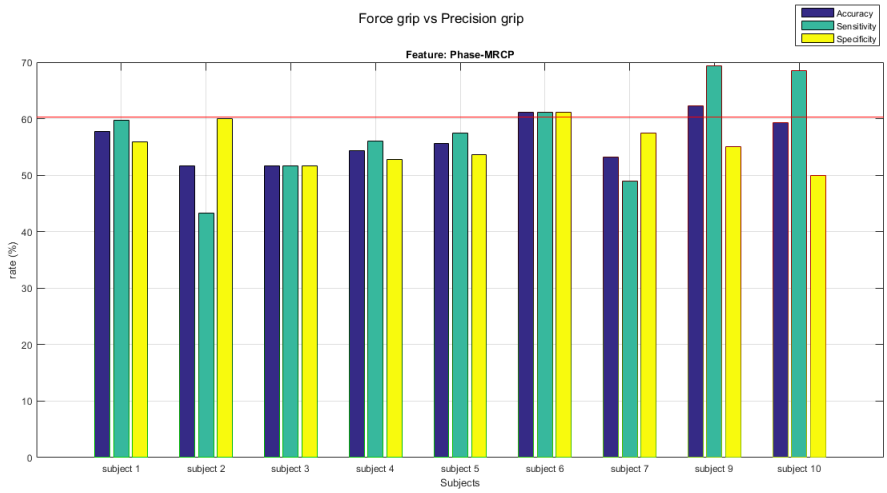

Figure 4.11: Classification results between force and precision grip using amplitude as feature.

DSP features

We extracted features obtained by filtering epochs with DSP filter. We retained the 2 rows of signals filtered. Feature vector was normalize in the range [0-1].
We compute DSP filter with the train data and then, the filter obtained, was applied to test data. The average decoding accuracy, using features obtained by filtering with DSP, was 64.89% (average for all subjects). The accuracy together with the sensitivity and specificity rate; obtained for each subject is shown in Fig.4.12

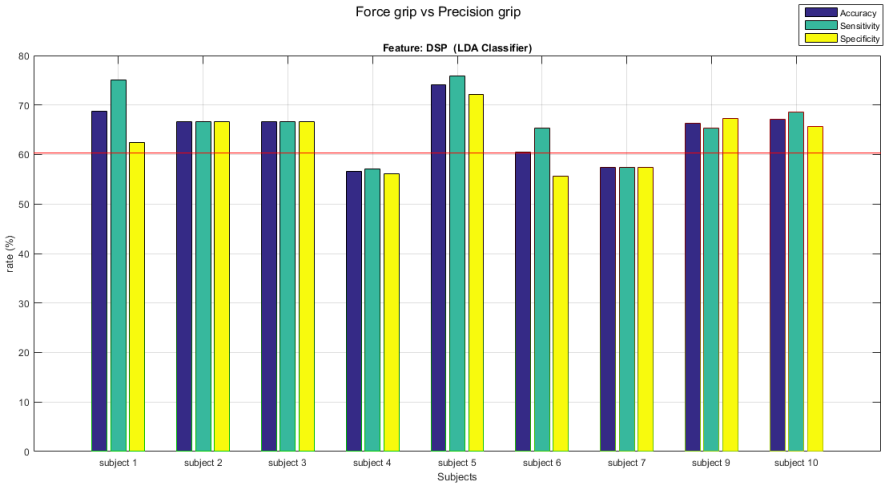

Figure 4.12: Classification results obtained for 9 subjects, using DSP features.

Features comparison

A comparison of the accuracy obtained using these three types of features, decoded with LDA is shown in Fig.4.14. A T-test was performed to know if these decoding differences was statistically significant ($p < 0.5\%$). Statistically significant differences were found for DSP features vs phase features. However, no significant differences were found between time features and DSP features.

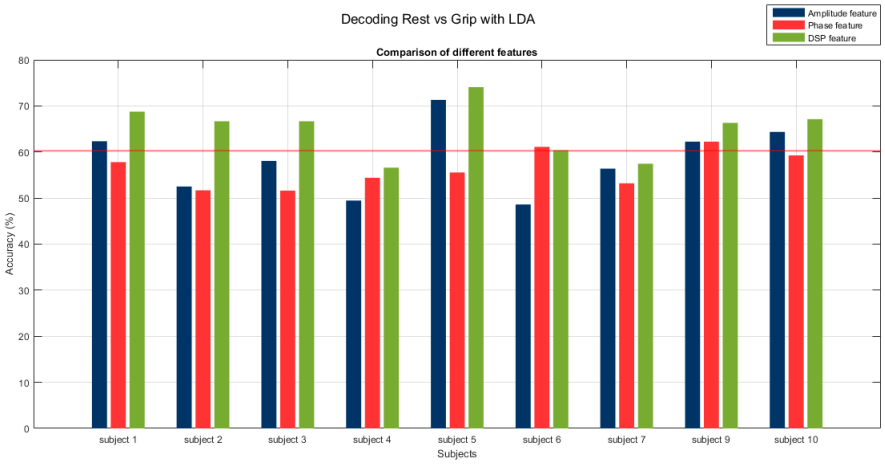

Figure 4.13: Comparison of accuracy obtained with each feature.

Decoding using a Support Vector Machine

For the case of DSP features, since a higher accuracy value was obtained with these features (although difference was no statistically significant), we use also a Support Vector Machine with Radial Basis Function (RBF) as kernel. Classification results obtained with SVM are shown next.

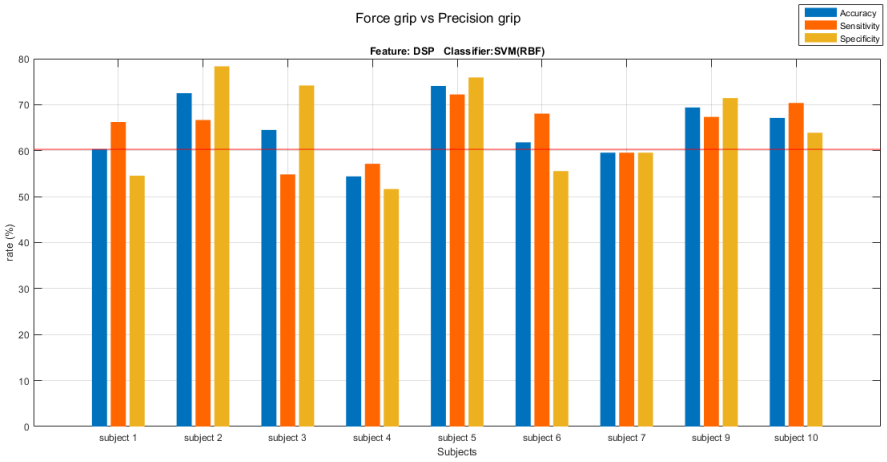

Figure 4.14: Classification results obtained by a SVM classifier using DSP features.

We have also a comparison for the same type of features (DSP-features) implementing two different classifiers (LDA and SVM)

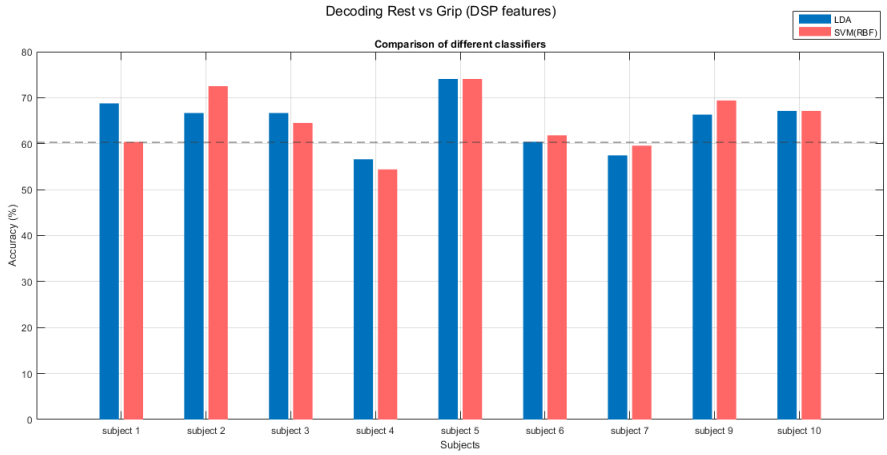

Figure 4.15: Classifiers comparison using DSP features.

Chapter 5

Discussion, Conclusion and Future work

5.1 Discussion

5.1.1 Pipeline integration

We discuss here each one of the preprocessing techniques implemented.

ASR cleaning. Although the strong capabilities cleaning EEG record, we did not contemplate this method in our pipeline. Its omission lies in the fact that signals channels are recomposed from their adjacent channels, so we could not observed MRCP morphology once this filter was applied. Since one of the aim in this thesis was EEG analysis regarding MRCP latencies and amplitudes, we did not take advantage of ASR cleaning.
We found that ASR implementation even has a strong impact when ICA need to be applied later. That is because the new reconstructed channels do not represent any more a linear span of sources. Despite of this fact, ASR reconstruction even deals with blink artifacts and some other artifacts commonly rejected with ICA. In our case, we reject these artifacts through frontal channels performing ICA. However, we found in ASR method a promising tools for EEG arrangement where no frontal channels are available or ICA does not achieve a desired artifact rejection.

Evaluation of different spatial filters. Results in our comparison of spatial filters shown good performance for CAR and small Laplace in terms of SNR. However, for a fair comparison sLaplace need to be applied in more channels. Even if we did not take into account, we suggest methodology here followed for selecting a spatial filter. Visual inspection of filter effects may lead to wrong results. An objectivity measure should take into account like SNR value among others.

Preprocessing towards MRCP Analysis. Filtering in a narrow window of 0.1-1 Hz may deal with must of common artifacts except for artifacts present in slow frequency. Since we reject these artifacts by ICA , these two techniques together with a threshold assured to us a good preprocessing pipeline for our task.

5.1.2 MRCP nature in grasping functional movements

The presence of more than one MRCP negative peaks during grasp functional activities as well as the temporal evolution with respect to different events have not been reported previously in studies concerning to grasp decode. A more strict experimental design and methodology need to be carry out to report conclusion from it. However, we believe that these preliminary results may contribute to the framework of motor decoding for BCI systems since they underline a promising hypothesis that the temporal resolution of EEG may provide specific decoding information about the stages developed in a functional movement.

5.1.3 time-lock to reach or grasp?

Among studies that aim classification of grasp types from EEG correlates, there is a discrepancy with respect to the event considered to time lock signals. While some studies take the moment of grasp as the event to time lock the signals, others consider the moment of reaching. Furthermore, studies that consider onset as the reaching time, point to grasp differences in amplitude. On the other hand, whereas grasp moment is taken as onset, some studies indicated that differences in grasp types are encoded in latency.
We evaluate both scenarios in our experiments, since our instrumentation allow us knowing the exact time in EEG recording when each movement stage is performed as well as time lock signals to each of these onset event. What we found is that some differences in latencies may appear depending on event considered to time lock signals. This is because time spent in performing force grips normally is faster than precision grips (see Fig.5.1). We compute differences of time spent for performing force grasp versus precision grasp.

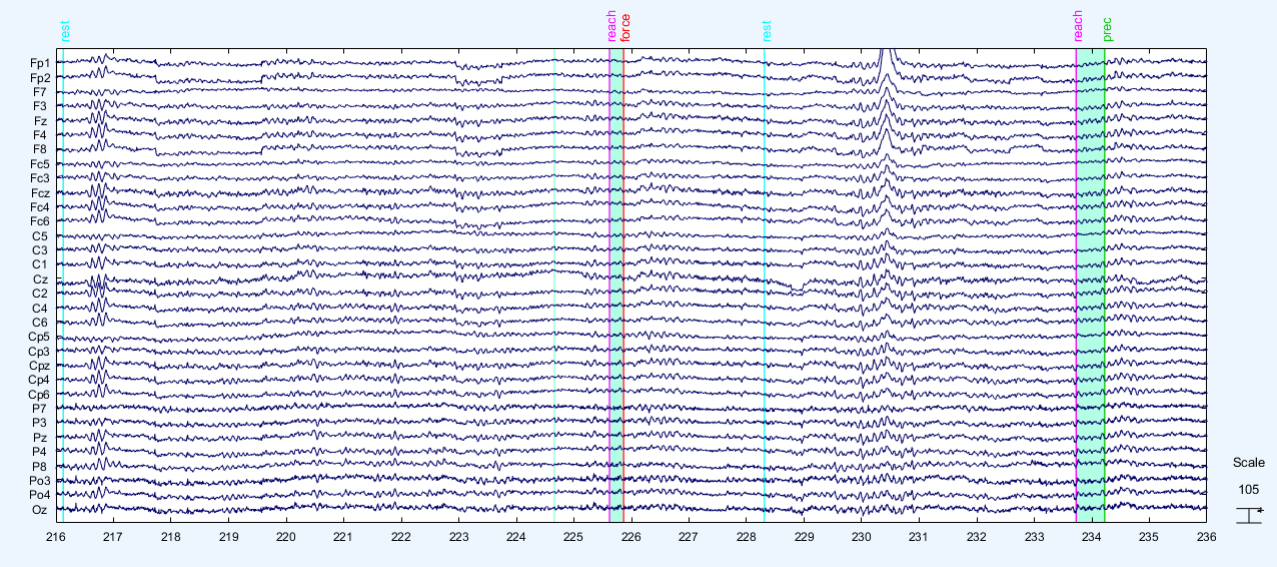

Figure 5.1: Comparison of time to perform force grasp vs precision grasp

We found that, for our experiment task, there is a difference of 200 ms.Differences in latency of negative peak MRCP from these two kinds of grasp may be due to time to be performed rather than a discriminative feature encoded. We suggest that this need to be considered when differences in latencies are assumed for other decoding of motor tasks.

It does not mean that time spent to perform and activity were not encode in brain signals. Actually, according to others neuroimaging studies[53], movements that required more attention and time (like precision grasp) activates different brain regions.

5.2 Conclusions

Neural correlates of grasping as functional movement

In this work, we have shown the existence of MRCP as neural correlates of grasping functional movements in self paced scenarios. It was concluded not only for the typical MRCP signal observed in the time locked signals but also for the results obtained in decoding rest vs grasp above chance level.

Implementation in neurorehabilitation

Discriminative differences between rest and grasp were found prior to reaching onset approximately 500 ms before.This also validate their implementation in neurorehabilitation therapies that involve detection of intention of grasp. It is significant for BCI oriented to neurorehabilitation therapies since timing involved in decoding and feedback sending by BCI system is crucial for succeed in enhancing brain plasticity.

Decoding grasp performed from EEG

Although some features exploited did not lead to classification results above empirical chance level. The good performance obtained by DSP features not only suggest that decoding of grasp type is possible, but also that grip type may be encode in MRCP amplitudes. We arrive to this conclusion because DSP is designed to improve classification results derived from time MRCP features.

5.3 Future works

Simulation of online performance

We may implement classification stage through a sliding window to simulate on-line performance of grasp decoding and assess the implementation of grasp decoding in the framework towards control of hand ortheses and prosthesis from high level commands, leading to a natural way of controlling these robotic devices.

Dry technology

We have implemented this experimental protocol with dry EEG technology, however results are not yet obtained. One of the challenges of BCI systems is get from the lab into real world usefulness. This might be possible if dry technology can be validated through its implementation in motor BCI systems.

Feature extraction from MRCP

There is an opening research in finding which MRCP features enconde motor information concerning to grasp functional movements.

Stroke patients

In thesis work, we found neural correlates of grasping and validate that decoding of grip performed is possible. However these results were obtained from healthy participants. Replicate this patWe have implemented this experimental protocol with dry EEG technology, however results are not yet obtained. Using this technology may also assess the use of these decoding systems out from the lab into the real life applications. For neurorehabilitation purposes is also important

Bibliography

[1] Benjamin, E. J., Blaha, M. J., Chiuve, S. E., Cushman, M., Das, S. R., Deo, R., ... & Isasi, C. R. (2017). Heart disease and stroke statistics—2017 update: a report from the American Heart Association. Circulation, 135(10), e146-e603.

[2] Thrift, A. G., Thayabaranathan, T., Howard, G., Howard, V. J., Rothwell, P. M., Feigin, V. L., ... & Cadilhac, D. A. (2017). Global stroke statistics. International Journal of Stroke, 12(1), 13-32. ISO 690

[3] Sultan, S., & Elkind, M. S. (2013). The growing problem of stroke among young adults. Current cardiology reports, 15(12), 421.

[4] Monge-Pereira, E., Ibañez-Pereda, J., Alguacil-Diego, I. M., Serrano, J. I., Spottorno-Rubio, M. P., & Molina-Rueda, F. (2017). Use of Electroencephalography Brain Computer Interface systems as a rehabilitative approach for upper limb function after a stroke. A systematic review. PM& R.

[5] Graimann, B., Allison, B. Z., & Pfurtscheller, G. (Eds.). (2010). Brain-computer interfaces: Revolutionizing human-computer interaction. Springer Science & Business Media.

[6] Wolpaw, J.R., Birbaumer, N., McFarland, D.J., Pfurtscheller, G., Vaughan, T.M.: Brain–computer interfaces for communication and control. Electroencephalogr. Clin. Neurophysiol.

[7] Rohm, M., Schneiders, M., Müller, C., Kreilinger, A., Kaiser, V., Müller-Putz, G. R., & Rupp, R. (2013). Hybrid brain–computer interfaces and hybrid neuroprostheses for restoration of upper limb functions in individuals with high-level spinal cord injury. Artificial intelligence in medicine, 59(2), 133-142.

[8] K. Lee, D. Liu, L. Perroud, R. Chavarriaga, J.d.R. Millan, A brain-controlled exoskeleton with cascaded event-related desynchronization classifiers, Robotics and Autonomous Systems (2016)

[9] Vidaurre, C., Sannelli, C., Muller, K.-R., Blankertz, B., 2011a. Co-adaptive calibration to improve BCI efficiency. J. Neural Eng. 8, 025009.

[10] Faller, J., et al., 2014. A co-adaptive brain–computer interface for end users with severe motor impairment. PLoS One 9 (7), 1–10.

[11] Schwarz, A., et al., 2015. A co-adaptive sensory motor rhythms brain–computer interface based on common spatial patterns and random forest. Conf. Proc. IEEE Eng. Med. Biol.Soc. 2015, 1049–1052.

[12] Yao, L., Sheng, X., Zhang, D., Jiang, N., Mrachacz-Kersting, N., Zhu, X., & Farina, D. (2017). A stimulus-independent hybrid BCI based on Motor Imagery and Somatosensory Attentional Orientation. IEEE Transactions on Neural Systems and Rehabilitation Engineering.

[13] Müller-Putz, G. R., Ofner, P., Schwarz, A., Pereira, J., Pinegger, A., Dias, C. L., ... & Sburlea, A. I. (2017, January). Towards non-invasive EEG-based arm/hand-control in users with spinal cord injury. In Brain-Computer Interface (BCI), 2017 5th International Winter Conference on (pp. 63-65). IEEE.

[14] Wolpaw, J. R., Loeb, G. E., Allison, B. Z., Donchin, E., do Nascimento, O. F., Heetderks, W. J., ... & Turner, J. N. (2006). BCI meeting 2005-workshop on signals and recording methods. IEEE Transactions on neural systems and rehabilitation engineering, 14(2), 138-141.

[15] Wang W, Collinger JL, Degenhart AD, Tyler-Kabara EC, Schwartz AB, Moran DW, et al. (2013) An Electrocorticographic Brain Interface in an Individual with Tetraplegia. PLoS ONE 8(2): e55344.

[16] Leuthardt, E. C., Gaona, C., Sharma, M., Szrama, N., Roland, J., Freudenberg, Z., ... & Schalk, G. (2011). Using the electrocorticographic speech network to control a brain–computer interface in humans. Journal of neural engineering, 8(3), 036004.

[17] Leuthardt, E. C., Schalk, G., Wolpaw, J. R., Ojemann, J. G., & Moran, D. W. (2004). A brain–computer interface using electrocorticographic signals in humans. Journal of neural engineering, 1(2), 63.

[18] Sitaram, R., Zhang, H., Guan, C., Thulasidas, M., Hoshi, Y., Ishikawa, A., Shimizu, K., and Birbaumer, N. Temporal classification of multichannel near-infrared spectroscopy signals of motor imagery for developing a brain–computer interface. Neuroimage 34, 1416–1427.

[19] S.P. Levine, J.E. Huggins et al. Identification of electrocorticogram patterns as the basis for a direct brain interface. J Clin Neurophysiol. 1999 Sep; 16(5):439-47.

[20] Donchin et al. Talking off the loop of your head: toward a mental prosthesis. Electroencephalogr Clin Neurophysiol. 1988 Dec; 70(6):510-23.

[21] Jasper, H.H.: The ten twenty electrode system of the international federation. Electroencephalogr. Clin. Neurophysiol. 10, 371–375 (1958)

[22] Schalk, G., & Mellinger, J. (2010). A practical guide to brain–computer interfacing with BCI2000: General-purpose software for brain-computer interface research, data acquisition, stimulus presentation, and brain monitoring (pp.17-18). Springer Science & Business Media.

[23] Muthukumaraswamy, S. D. (2013). High-frequency brain activity and muscle artifacts in MEG/EEG: a review and recommendations. Frontiers in human neuroscience, 7.

[24] Gu, Y., Dremstrup, K., & Farina, D. (2009). Single-trial discrimination of type and speed of wrist movements from EEG recordings. Clinical Neurophysiology, 120(8), 1596-1600.

[25] Jochumsen, M., Niazi, I.K., Mrachacz-Kersting, N., Farina, D., Dremstrup, K., 2013. Detection and classification of movement-related cortical potentials associated with task force and speed. J. Neural Eng. 10, 056015.

[26] López-Larraz, E., Montesano, L., Gil-Agudo, Á., & Minguez, J. (2014). Continuous decoding of movement intention of upper limb self-initiated analytic movements from pre-movement EEG correlates. Journal of neuroengineering and rehabilitation, 11(1), 153.

[27] Rizzolatti, G., Cattaneo, L., Fabbri-Destro, M., Rozzi, S., 2014. Cortical mechanisms underlying the organization of goal-directed actions and mirror neuron-based action understanding. Physiol. Rev. 94, 655–706.

[28] Pereira, J., Ofner, P., Schwarz, A., Sburlea, A. I., & Müller-Putz, G. R. (2017). EEG neural correlates of goal-directed movement intention. NeuroImage, 149, 129-140.

[29] Ofner, P., & Müller-Putz, G. R. (2015, August). Movement target decoding from EEG and the corresponding discriminative sources: A preliminary study. In Engineering in Medicine and Biology Society (EMBC), 2015 37th Annual International Conference of the IEEE (pp. 1468-1471). IEEE.

[30] Úbeda, A., Azorín, J. M., Chavarriaga, R., & Millán, J. D. R. (2017). Classification of upper limb center-out reaching tasks by means of EEG-based continuous decoding techniques. Journal of neuroengineering and rehabilitation, 14(1), 9.

[31] Bradberry, T. J., Gentili, R. J., & Contreras-Vidal, J. L. (2010). Reconstructing three-dimensional hand movements from noninvasive electroencephalographic signals. Journal of Neuroscience, 30(9), 3432-3437.

[32] Ofner, P., & Müller-Putz, G. R. (2012, August). Decoding of velocities and positions of 3D arm movement from EEG. In Engineering in Medicine and Biology Society (EMBC), 2012 Annual International Conference of the IEEE (pp. 6406-6409). IEEE.

[33] Antelis, J. M., Montesano, L., Ramos-Murguialday, A., Birbaumer, N., & Minguez, J. (2013). On the usage of linear regression models to reconstruct limb kinematics from low frequency EEG signals. PLoS One, 8(4), e61976.

[34] Sburlea, A. I., Montesano, L., de la Cuerda, R. C., Diego, I. M. A., Miangolarra-Page, J. C., & Minguez, J. (2015). Detecting intention to walk in stroke patients from pre-movement EEG correlates. Journal of neuroengineering and rehabilitation, 12(1), 113.

[35] Melinscak, F., Montesano, L., & Minguez, J. (2016). Asynchronous detection of kinesthetic attention during mobilization of lower limbs using EEG measurements. Journal of neural engineering, 13(1), 016018.

[36] Velu, P. D., & de Sa, V. R. (2013). Single-trial classification of gait and point movement preparation from human EEG. Frontiers in neuroscience, 7.

[37] López-Larraz, E., Trincado-Alonso, F., Rajasekaran, V., Pérez-Nombela, S., del-Ama, A. J., Aranda, J., ... & Montesano, L. (2016). Control of an ambulatory exoskeleton with a brain–machine interface for spinal cord injury gait rehabilitation. Frontiers in neuroscience, 10.

[38] Sburlea, A. I., Montesano, L., & Minguez, J. (2015). Continuous detection of the self-initiated walking pre-movement state from EEG correlates without session-to-session recalibration. Journal of neural engineering, 12(3), 036007.

[39] Li, Y., Ang, K. K., & Guan, C. (2009). Digital signal processing and machine learning. In Brain-Computer Interfaces (pp. 305-330). Springer Berlin Heidelberg.

[40] Wolpaw, J. R., Birbaumer, N., McFarland, D. J., Pfurtscheller, G., & Vaughan, T. M. (2002). Brain–computer interfaces for communication and control. Clinical neurophysiology, 113(6), 767-791.

[41] Niedermeyer, E., & da Silva, F. L. (Eds.). (2005). Electroencephalography: basic principles, clinical applications, and related fields. Lippincott Williams & Wilkins.

[42] Ball, T., Demandt, E., Mutschler, I., Neitzel, E., Mehring, C., Vogt, K., ... & Schulze-Bonhage, A. (2008). Movement related activity in the high gamma range of the human EEG. Neuroimage, 41(2), 302-310.

[43] Wang, Y., Gao, X., Hong, B., & Gao, S. (2009). Practical designs of brain–computer interfaces based on the modulation of EEG rhythms. In Brain-Computer Interfaces (pp. 137-154). Springer Berlin Heidelberg.

[44] Kornhuber, H. H., & Deecke, L. (1965). Hirnpotentialänderungen bei Willkürbewegungen und passiven Bewegungen des Menschen: Bereitschaftspotential und reafferente Potentiale. Pflügers Archiv European Journal of Physiology, 284(1), 1-17.

[45] Shibasaki, H., & Hallett, M. (2006). What is the Bereitschaftspotential?. Clinical neurophysiology, 117(11), 2341-2356.

[46] Steyrl, D., Scherer, R., Faller, J., & Müller-Putz, G. R. (2016). Random forests in non-invasive sensorimotor rhythm brain-computer interfaces: a practical and convenient non-linear classifier. Biomedical Engineering/Biomedizinische Technik, 61(1), 77-86.

[47] Quitadamo, L. R., Cavrini, F., Sbernini, L., Riillo, F., Bianchi, L., Seri, S., & Saggio, G. (2017). Support vector machines to detect physiological patterns for EEG and EMG-based human–computer interaction: a review. Journal of neural engineering, 14(1), 011001.

[48] Obermaier, B., Guger, C., Neuper, C., & Pfurtscheller, G. (2001). Hidden Markov models for online classification of single trial EEG data. Pattern recognition letters, 22(12), 1299-1309.

[49] Napier, J. R. Studies of the hands of living primates. Proc. Zool. Soc. 134, 647–657 (1960).

[50] Castiello, U. (2005). The neuroscience of grasping. Nature reviews. Neuroscience, 6(9), 726.

[51] Turella, L., & Lingnau, A. (2014). Neural correlates of grasping. Frontiers in human neuroscience, 8.

[52] Popovic, D. B., & Sinkjær, T. (2008). Central nervous system lesions leading to disability. Journal of Automatic Control, 18(2), 11-23.

[53] H. Ehrsson, A. Fagergren, T. Jonsson, G. Westling, R. Johansson, H. Forssberg, Cortical activity in precision-versus power-grip tasks: An fMRI study, Journal of Neurophysiology 83 (1) (2000) 528-536.

[54] Davare, M., Andres, M., Cosnard, G., Thonnard, J. L., & Olivier, E. (2006). Dissociating the role of ventral and dorsal premotor cortex in precision grasping. Journal of Neuroscience, 26(8), 2260-2268.

[55] Battaglia-Mayer,A.,Archambault,P.S.,and Caminiti,R.(2006).The network for eye hand coordination and its relevance to understanding motor disorders of parietal patients. Neuropsychologia

[56] Fattori,P.,Breveglieri,R.,Raos,V.,Bosco,A.,and Galletti,C.(2012).Vision for action in the macaque medial posterior parietal cortex. J. Neurosci. 32, 3221– 3234.

[57] Fabbri, S., Strnad, L., Caramazza, A., and Lingnau, A.(2014).Overlapping representations for grip type and reach direction. Neuroimage 94, 138–146.

[58] Feix, T., Romero, J., Schmiedmayer, H. B., Dollar, A. M., & Kragic, D. (2016). The grasp taxonomy of human grasp types. IEEE Transactions on Human-Machine Systems, 46(1), 66-77.

[59] Agashe, H. A., Paek, A. Y., Zhang, Y., & Contreras-Vidal, J. L. (2015). Global cortical activity predicts shape of hand during grasping. Frontiers in neuroscience, 9.

[60] Pistohl, T., Schulze-Bonhage, A., Aertsen, A., Mehring, C., & Ball, T. (2012). Decoding natural grasp types from human ECoG. Neuroimage, 59(1), 248-260.

[61] Pistohl, T., Schmidt, T. S. B., Ball, T., Schulze-Bonhage, A., Aertsen, A., & Mehring, C. (2013). Grasp detection from human ECoG during natural reach-to-grasp movements. PloS one, 8(1), e54658.

[62] Jochumsen, M., Rovsing, C., Rovsing, H., Niazi, I. K., Dremstrup, K., & Kamavuako, E. N. (2017). Classification of Hand Grasp Kinetics and Types Using Movement-Related Cortical Potentials and EEG Rhythms. Computational Intelligence and Neuroscience, 2017.

[63] Iturrate, I., Leeb, R., Chavarriaga, R., & Millán, J. D. R. (2016). Decoding of two hand grasping types from EEG. In Proceedings of the 6th International Brain-Computer Interface Meeting (No. EPFL-CONF-218934).

[64] Randazzo, L., Iturrate, I., Chavarriaga, R., Leeb, R., & Millán, J. D. R. (2015, August). Detecting intention to grasp during reaching movements from EEG. In Engineering in Medicine and Biology Society (EMBC), 2015 37th Annual International Conference of the IEEE (pp. 1115-1118). IEEE.

[65] Schwarz, A., Schwarz, A., & Ofner, P. (2016). Time domain classification of grasp and hold tasks. In Proceedings of the 6th International Brain–computer Interface Meeting (p. 76).

[66] Muller-Putz, G. R., Ofner, P., Schwarz, A., Pereira, J., Pinegger, A., Dias, C. L., ... & Sburlea, A. I. (2017, January). Towards non-invasive EEG-based arm/hand-control in users with spinal cord injury. In Brain-Computer Interface (BCI), 2017 5th International Winter Conference on (pp. 63-65). IEEE.

[67] Delorme, A., Makeig, S., 2004. EEGLAB: an open source toolbox for analysis of single trial EEG dynamics including independent component analysis. J. Neurosci.Methods 134, 9–21

[68] Bell, A. J., & Sejnowski, T. J. (1995). An information-maximization approach to blind separation and blind deconvolution. Neural computation, 7(6), 1129-1159.

[69] Mullen, T. R., Kothe, C. A., Chi, Y. M., Ojeda, A., Kerth, T., Makeig, S., ... & Cauwenberghs, G. (2015). Real-time neuroimaging and cognitive monitoring using wearable dry EEG. IEEE Transactions on Biomedical Engineering, 62(11), 2553-2567.

[70] Jochumsen, M., Niazi, I. K., Mrachacz-Kersting, N., Jiang, N., Farina, D., & Dremstrup, K. (2015). Comparison of spatial filters and features for the detection and classification of movement-related cortical potentials in healthy individuals and stroke patients. Journal of neural engineering, 12(5), 056003.

[71] Liao, X., Yao, D., Wu, D., & Li, C. (2007). Combining spatial filters for the classification of single-trial EEG in a finger movement task. IEEE Transactions on Biomedical Engineering, 54(5), 821-831.

[72] Sburlea, A. I., Montesano, L., & Minguez, J. (2017). Advantages of EEG phase patterns for the detection of gait intention in healthy and stroke subjects. Journal of Neural Engineering, 14(3), 036004.

[73] Canolty, R. T., Cadieu, C. F., Koepsell, K., Ganguly, K., Knight, R. T., & Carmena, J. M. (2012). Detecting event-related changes of multivariate phase coupling in dynamic brain networks. Journal of neurophysiology, 107(7), 2020-2031.

[74] Lachaux, J. P., Rodriguez, E., Martinerie, J., & Varela, F. J. (1999). Measuring phase synchrony in brain signals. Human brain mapping, 8(4), 194-208.

[75] Fabien Lotte, Marco Congedo, Anatole Lécuyer, Fabrice Lamarche, Bruno Arnaldi. A review of classification algorithms for EEG-based brain computer interfaces. Journal of Neural Engineering, IOP Publishing, 2007, 4, pp.24.

[76] Combrisson E, Jerbi K. Exceeding chance level by chance: The caveat of theoretical chance levels in brain signal classification and statistical assessment of decoding accuracy. J Neurosci Methods (2015)